



From the Transantarctic Basin to the Ferrar Large Igneous Province—New palynostratigraphic age constraints for Triassic–Jurassic sedimentation and magmatism in East Antarctica

Benjamin Bomfleur^{a,*}, Robert Schöner^{b,2}, Jörg W. Schneider^{c,d}, Lothar Viereck^e, Hans Kerp^a, John L. McKellar^f

^a Forschungsstelle für Paläobotanik am Institut für Geologie und Paläontologie, Westfälische Wilhelms-Universität Münster, Heisenbergstraße 2, D-48149 Münster, Germany

^b GeoZentrum Nordbayern, Friedrich-Alexander-Universität Erlangen-Nürnberg, Schlossgarten 5, D-91054 Erlangen, Germany

^c Institut für Geologie, TU Bergakademie Freiberg, Bernhard-von-Cotta Straße 2, D-09596 Freiberg, Germany

^d Kazan Federal University, 18 Kremlevskaya Str., Kazan 420008, Russian Federation

^e Institut für Geowissenschaften, Friedrich-Schiller-Universität Jena, Burgweg 11, D-07749 Jena, Germany

^f Geological Survey of Queensland, Department of Natural Resources and Mines, PO Box 15216, City East, Brisbane, Queensland 4002, Australia

ARTICLE INFO

Article history:

Received 7 October 2012

Received in revised form 10 February 2014

Accepted 3 April 2014

Available online 24 April 2014

Keywords:

Beacon Supergroup

Ferrar Province

Classopollis

Alisporites

Palynostratigraphy

Transantarctic Mountains

ABSTRACT

We present new palynological data from the Transantarctic Mountains that clarify the timing of sedimentary and magmatic processes in the transition from continental deposition of the Beacon Supergroup to emplacement of the Ferrar Large Igneous Province. Samples were collected from twenty-three Triassic and Jurassic sections in the southern area of north Victoria Land (NVL), East Antarctica. Recovered palynomorph assemblages are correlated with the widely used, although informal palynostratigraphic framework established for eastern Australia by Price. The associated Late Triassic–earliest Jurassic zone, APT5, is modified here with a proposed new subdivision: Lower APT5 (“APT5L”; middle–late Norian), Middle APT5 (“APT5M”; Rhaetian), and Upper APT5 (“APT5U”; Hettangian–earliest Sinemurian). We further propose a modification unifying the relevant formal eastern Australian and New Zealand palynostratigraphic zones, with a new *Polycingulatisporites crenulatus* Association Zone (new zonal status) that includes the *P. crenulatus* Association Subzone (new subzone; equivalent to APT5L) and the following *Foveosporites moretonensis* Association Subzone (new subzonal status; equivalent to APT5M). Our palynostratigraphic dating of the NVL assemblages demonstrates that the onset of sedimentation was diachronous in this part of the Transantarctic Basin, ranging from at least the Rhaetian to, in places, early Sinemurian. By lack of evidence for rocks containing APT5U assemblages and by analogy with the few coeval sections in Australia, we infer that the Hettangian interval in NVL is probably consumed by unconformity. Deposition of ashes from distal silicic volcanism commenced in the early Sinemurian and reached a peak phase beginning in middle Pliensbachian (ca 187 Ma), coinciding with the first major magmatic interval of the silicic Chon Aike Province in Patagonia and West Antarctica. Two major episodes of phreatomagmatic activity, driven by shallow-level sill intrusion into sandstone aquifers, occurred during the middle Pliensbachian and during the late Pliensbachian–early Toarcian. The latter episode was closely followed by the first pillow extrusion and local lava effusion. Contrary to some previous studies, we further conclude that all available palynological evidence is compatible with a short-lived emplacement of the plateau-forming Kirkpatrick Basalt at around 180 Ma during the early Toarcian.

© 2014 Elsevier B.V. All rights reserved.

1. Introduction

The Transantarctic Basin developed at the Panthalassan margin of eastern Gondwana during the mid-Palaeozoic and persisted until the

initial stage of Gondwana break-up in the Early Jurassic (see, e.g., Barrett, 1991; Elliot, 2013). The basin contains a succession of Devonian to Jurassic deposits referred to as the Beacon Supergroup. Today, exposures of this supergroup occur in north and south Victoria Land (NVL and SVL), in the central Transantarctic Mountains (CTM), and in isolated outcrop areas along the perimeter of the East Antarctic craton, including the Ellsworth, Pensacola, and Theron mountains (EM, PM, TM) (Barrett, 1991; Collinson et al., 1994) (Fig. 1). The central parts of the Transantarctic Basin (encompassing EM, CTM, and SVL) contain thick mid–late Palaeozoic sequences, including Devonian marine deposits and Carboniferous–Permian glacial and fluvio-lacustrine

* Corresponding author.

E-mail address: benjamin.bomfleur@nrm.se (B. Bomfleur).

¹ Present address: Department of Palaeobiology, Swedish Museum of Natural History, Box 50007, SE 104 05 Stockholm, Sweden.

² Present address: Zentrum für TiefenGeothermie/Oberflächennahe Geothermie, Landesamt für Bergbau, Energie und Geologie (LBEG), Hannoversche Straße 30A, D-29221 Celle, Germany.

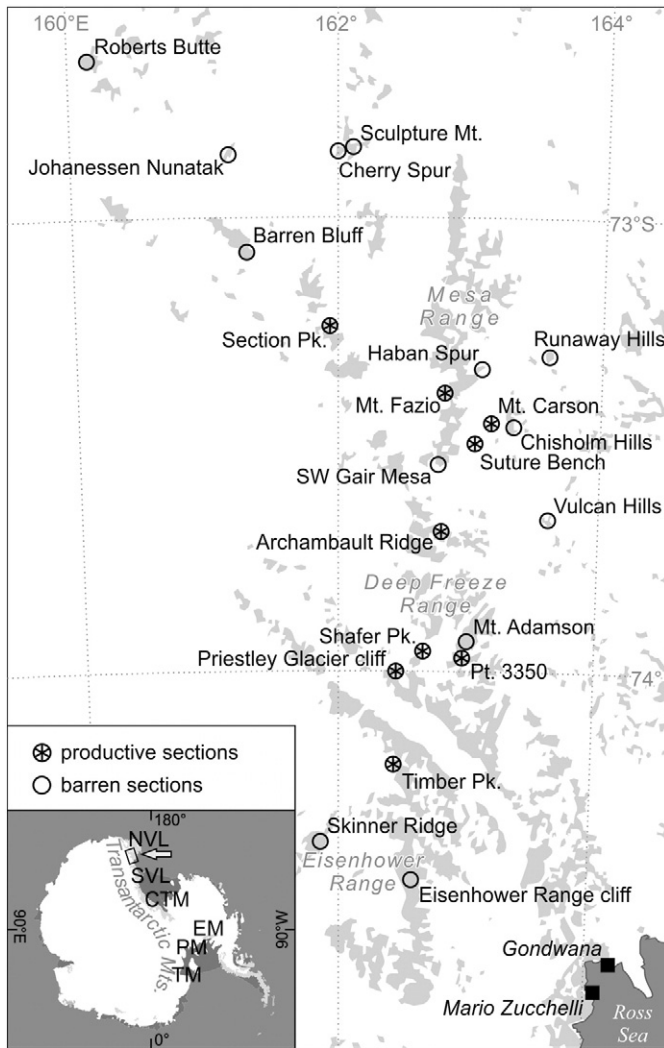


Fig. 1. Map showing the study area and sections sampled during GANOVEX IX (2005/2006); samples from Mount Fazio, Cherry Spur, Haban Spur, and Sculpture Mountain were collected during the 1981/1982 US–New Zealand–Australia Joint International Expedition.

deposits (Collinson et al., 1994). Following Early Triassic reversal in palaeoslope direction towards Australia, a more or less uniform fluvial depositional system developed throughout the central to eastern part of the Transantarctic Basin (CTM to NVL) (Barrett, 1991; Collinson et al., 1994).

The initiation of Gondwana break-up during the Early Jurassic is recorded in the Transantarctic Mountains (TAM) with the formation of the Ferrar Large Igneous Province, which produced a thick succession (>1000 m) of flood basalts (Kirkpatrick Basalt) and related sill- and dike intrusions (Ferrar Dolerite) (Elliot and Fleming, 2008; Elliot, 2013). Present exposures of the Ferrar Group extend over more than 3000 km from East Antarctica into Tasmania (e.g., Elliot and Fleming, 2008). Where the volcanic succession is preserved, it is underlain by mafic volcanoclastic deposits that originated during violent, explosive water–magma interactions when early-ascending sill intrusions intersected host-rock aquifers (e.g., Hanson and Elliot, 1996; White and McClintock, 2001; McClintock and White, 2006; Viereck-Goette et al., 2007). The volcanoclastic deposits occur not only in the form of phreatomagmatic vent-complex and diatreme infillings that cut into the sedimentary succession (e.g., Hanson and Elliot, 1996; McClintock and White, 2006), but also as stratified, conformably

intercalated extra-vent deposits, i.e., air-fall, surge, and flow deposits (e.g., Viereck-Goette et al., 2007; Elliot and Fleming, 2008). A remarkable feature of the Ferrar Province is its association with intense silicic volcanism that preceded flood-basalt effusion, which is documented by successions of rhyolitic tuffs and tuffitic sandstones and siltstones that are locally preserved below the Kirkpatrick Basalt throughout the TAM (Elliot, 1996, 2000; Schöner et al., 2007; Elliot, 2013) and below its equivalents in Tasmania (Bromfield et al., 2007). These successions are interpreted as distal products from (ultra-)Plinian eruptions of a presently unidentified Early Jurassic volcanic centre, which may have been located in West Antarctica or in an unexposed crustal terrain of the TAM (Elliot et al., 2007; Schöner et al., 2007).

Independent radiometric datings of Kirkpatrick Basalt from various localities throughout the TAM cluster tightly around ca 180 Ma (early Toarcian), which is interpreted as the period of peak magmatic activity (Pálffy and Smith, 2000; Riley and Knight, 2001). The timing of individual geodynamic processes in the Transantarctic Basin prior to flood-basalt effusion, however, is still not well understood, because the biostratigraphic framework for Mesozoic rocks in the TAM has so far remained poorly defined (e.g., Collinson, 1990; Askin and Cully, 1998). Initially, an exclusively Triassic age was assumed for the Mesozoic part of the Beacon Supergroup. An informal palynostratigraphic zonation for SVL and the CTM was proposed by Kyle (1977) and Kyle and Schopf (1982). The latter authors established a late Early to Late Triassic *Alisporites* Zone to contain Mesozoic strata of the Beacon Supergroup, and recognised four subzones (subzones A–D). Well-preserved Triassic palynomorph assemblages from the CTM were subsequently described by Farabee et al. (1989, 1990) and Askin and Cully (1998).

The first report of a Jurassic palynological assemblage in the TAM was already published by Gair et al. (1965) and Norris (1965). This assemblage, from fine-grained intercalations within a succession of quartzose sandstones at Section Peak, NVL, indicates an Early Jurassic age for the youngest deposits of the Beacon Supergroup (Norris, 1965; Pertusati et al., 2006). Recently published radiometric ages of detrital zircons from Section Peak confirm this age assignment (Goodge and Fanning, 2010; Elsner et al., 2013). Palynological data from the overlying volcanoclastic deposits are sparse and have yielded controversial results (see Tasch and Lammons, 1978; Shang, 1997; Musumeci et al., 2006; Ribecai, 2007). A major break in sedimentation between deposition of mafic volcanoclastics and the effusion of the Kirkpatrick Basalt has been suggested based on a well-preserved palynoflora from carbonaceous shale above pyroclastic breccias at Shafer Peak (Musumeci et al., 2006). Furthermore, palynofloras were described from lacustrine interbeds between lava flows at Carapace Nunatak, Storm Peak, and Coalsack Bluff (Tasch and Lammons, 1978); some of these assemblages have been interpreted as indicating a late Middle Jurassic age (Shang, 1997; Ribecai, 2007), which is incompatible with radiometric age constraints on the timing of lava emplacement (see Pálffy and Smith, 2000; Riley and Knight, 2001; Elliot, 2013).

We here present newly recovered palynological assemblages from NVL that (1) date the local onset of sedimentation for the first time; (2) provide a refined stratigraphic framework for epiclastic and volcanoclastic sedimentary units; and (3) enable dating of the individual phases of magmatic activity in the Ferrar Large Igneous Province.

2. Geological setting of the study area

In the southern region of NVL (Fig. 1), almost horizontally-lying deposits of the Beacon Supergroup sediments rest unconformably on pre-Devonian metamorphic and granitic basement, and are overlain by the Jurassic Kirkpatrick Basalt. The entire sedimentary succession is only ca 250–300 m thick, and consists of the Section Peak Formation, the Shafer Peak Formation (Collinson et al., 1986; Schöner et al., 2007), and multiple intercalated mafic volcanoclastic deposits related to phreatomagmatic activity [Exposure Hill Formation of Elliot et al. (1986a); here referred to as “Exposure Hill-type deposits” (Viereck-

Goette et al., 2007)]. In addition, putative glacial tillites and overlying successions of predominantly trough cross-bedded conglomerate and sandstone in the Eisenhower Range (Fig. 1), previously interpreted as basal portions of the Section Peak Formation (Casnedi and Di Giulio, 1999; Schöner et al., 2011), have been recently identified as new, still unnamed Palaeozoic deposits (Bomfleur et al., 2014).

The Section Peak Formation (up to ca 200 m thick) is composed largely of medium- to coarse-grained, trough cross-bedded fluvial sandstone (Collinson et al., 1986; Schöner et al., 2011). At Archambault Ridge, sandstone and thin conglomeratic layers overlie small depressions in the granitic basement that are locally filled with carbonaceous sandy pelites. Fine-grained intercalations, including fossiliferous siltstone and coal, are common in the upper part of the formation. In the Deep Freeze Range area (Fig. 1), the upper Section Peak Formation consists of a succession of at least five thick, bench-forming sandstone sheets with interbedded siltstone, claystone, and coal. Fossiliferous fine-grained deposits also occur at Timber Peak, Section Peak, Vulcan Hills, and Runaway Hills (Tessensohn and Mädlar, 1987; Bomfleur and Kerp, 2010a; Bomfleur et al., 2011a; Schöner et al., 2011). The first intercalations of silicic tuff occur in the uppermost part of the formation (Schöner et al., 2007). The age of the Section Peak Formation is currently considered to be Middle Triassic to Early Jurassic, based on macrofloras, palynological assemblages, and detrital-zircon ages (Gair et al., 1965; Norris, 1965; Tessensohn and Mädlar, 1987; Collinson et al., 1994; Casnedi and Di Giulio, 1999; Pertusati et al., 2006; Goodge and Fanning, 2010). The formation is interpreted as deposits of a sand-dominated, braided alluvial plain with paludal and lacustrine overbank environments. It has been suggested to correspond to the Falla and upper Lashly formations of the CTM and SVL (Kyle and Schopf, 1982; Collinson et al., 1994; Schöner et al., 2007, 2011).

The Section Peak Formation is conformably overlain by the Shafer Peak Formation, a ca 50-m-thick succession of homogeneous, light-grey, tuffitic siltstones and fine-grained sandstones (Schöner et al., 2007). Thin intercalations (up to 1 m thick) of olive-green to dark-grey, silty claystone occur locally. Relatively rich and diverse plant-fossil assemblages have been described from Shafer Peak and the Mount Carson area (Bomfleur and Kerp, 2010b; Bomfleur et al., 2011a,b). The Shafer Peak Formation is interpreted as comprising large volumes of silicic volcanic ash falls that were reworked in a fluvial environment (Schöner et al., 2007). Similar silicic tuffs and tuffitic deposits were reported from the upper part of the Early Jurassic Hanson Formation in the CTM (Elliot, 1996), and occur also in SVL in the form of a ca 47-m-thick unnamed unit (Elliot et al., 2007) and of megaclasts in mafic volcanoclastic breccias (Bradshaw, 1987; Elliot and Grimes, 2011).

Mafic volcanoclastic deposits in NVL have been described as the Exposure Hill Formation (Elliot et al., 1986a), a succession of subaqueous to subaerial, primary and reworked mafic pyroclastic rocks (Elliot et al., 1986a; Wörner, 1992). In the Mesa and Deep Freeze ranges, these mafic pyroclastic deposits form the fillings of local phreatomagmatic vent complexes (diatremes) that may be capped by pyroclast-rich lacustrine black shales, and also occur in the form of conformably intercalated extra-vent deposits that are concentrated at two stratigraphic levels: at the base and at the top of the Shafer Peak Formation (Schöner et al., 2007; Viereck-Goette et al., 2007) (Fig. 2). Therefore, following Viereck-Goette et al. (2007; see Elliot, 2013), we here refer to these units as lower and upper Exposure Hill-type deposits to discriminate their stratigraphic position. Musumeci et al. (2006) inferred a late Sinemurian to earliest Pliensbachian age for these deposits, based on a palynoflora from Shafer Peak.

The base of the overlying Kirkpatrick Basalt is locally characterized by pillow lavas (e.g., at Mount Adamson, Suture Bench, and Mount Carson; Viereck-Goette et al., 2007) (Figs. 1, 2). The lowermost, local lava flows are in places separated from the overlying plateau-lava successions by fluvio-lacustrine, fossiliferous sedimentary interbeds (e.g., at Mount Fazio and at the south-western end of Gair Mesa; Elliot et al., 1986b; Bomfleur et al., 2011a).

3. Samples and methods

Fifty-seven palynological samples from twenty-three outcrops in southern NVL were processed (Fig. 1). Most samples were collected during the “Ninth German Antarctic North Victoria Land Expedition (GANOVEX IX, 2005/2006)”. Six additional samples, kindly provided by D.H. Elliot (Columbus, OH), were collected from sedimentary interbeds between Kirkpatrick Basalt flows at Cherry Spur, Sculpture Mountain, Haban Spur, and Mount Fazio during the 1981–1982 US–New Zealand–Australia Joint International Expedition.

The amount of sediment processed varied from 5 to 15 g, depending on grain size and organic content; in one case (sample SHC32), we analysed the residues of a large macroscopic sample that was bulk-macerated for analysis of dispersed cuticles (see Bomfleur et al., 2011b). Hydrofluoric acid (48% HF at room temperature) was used for generally three to five days to dissolve mineral matter. In order to minimize mechanical destruction, samples were then neutralized manually (i.e., without centrifugation) by adding distilled water and careful decanting once residues were settled. This process was repeated until sample pH was neutral, usually after four to five rinses. The organic residues were then treated with Schulze's reagent [nitric acid (HNO₃) with a few crystals of potassium chlorate (KClO₃)]; the best results were achieved using Schulze's reagent with highly concentrated nitric acid (up to 60%; at room temperature) for only a short time span of 1 to 3 h. Following this treatment, the material was cleaned and bleached using 4% potassium hydroxide (KOH) for a few seconds. Samples were sieved over a 15 µm mesh screen. For the subsequent density separation, sodium polytungstate with a density of $d = 2$ was used. Glycerine jelly was used as the mounting medium for the preparation of slides for light-microscopical analysis.

Sample preparations were analysed with a Leica Diaplan microscope with Nomarski interference contrast. Photomicrographs were taken with a Nikon DS-5M digital camera; all specimen illustrations are composite micrographs, each being merged manually from several individual images taken at different focal planes in order to enhance sharpness (Bercovici et al., 2009; Kerp and Bomfleur, 2011). All material is housed in the Forschungsstelle für Paläobotanik at the Institut für Geologie und Paläontologie, Westfälische Wilhelms-Universität Münster, Germany.

Absolute ages of biostratigraphic zones were extrapolated correlating the modified informal biostratigraphic zonation of Price (Fig. 7.2 of McKellar in Cook et al., 2013) to the current version of the International Chronostratigraphic Chart of the International Commission of Stratigraphy (2013 v. 1; <http://www.stratigraphy.org>).

4. Sample yield and palynostratigraphy

Nineteen of the 57 processed samples yielded non-marine palynomorph assemblages; the remaining 38 samples were barren. The recorded assemblages were assessed biostratigraphically using the informal, alphanumeric spore-pollen zonation of Price (1997). This scheme, based on that of Price et al. (1985), and other antecedents referred to by Price (1997), is the most widely used palynostratigraphic zonation for the Mesozoic of eastern Gondwana. Although it has been repeatedly modified and refined (see Cook et al., 2013), further modifications to it are effected below with respect to the zonation of the Late Triassic–earliest Jurassic. In parallel with these amendments, the formal zonal schemes for the Late Triassic–earliest Jurassic of New Zealand and eastern Australia are amalgamated and also variously modified.

4.1. Palynostratigraphic zonation

For palynostratigraphic assessment of the productive material recovered from NVL, Price's (1997) scheme has been utilised, although modified here. As ages were only broadly assigned at the Epoch level by Price for his Jurassic units, the finer geochronologic subdivisions (at Age level) associated with them by McKellar (e.g., in Cook et al., 2013;

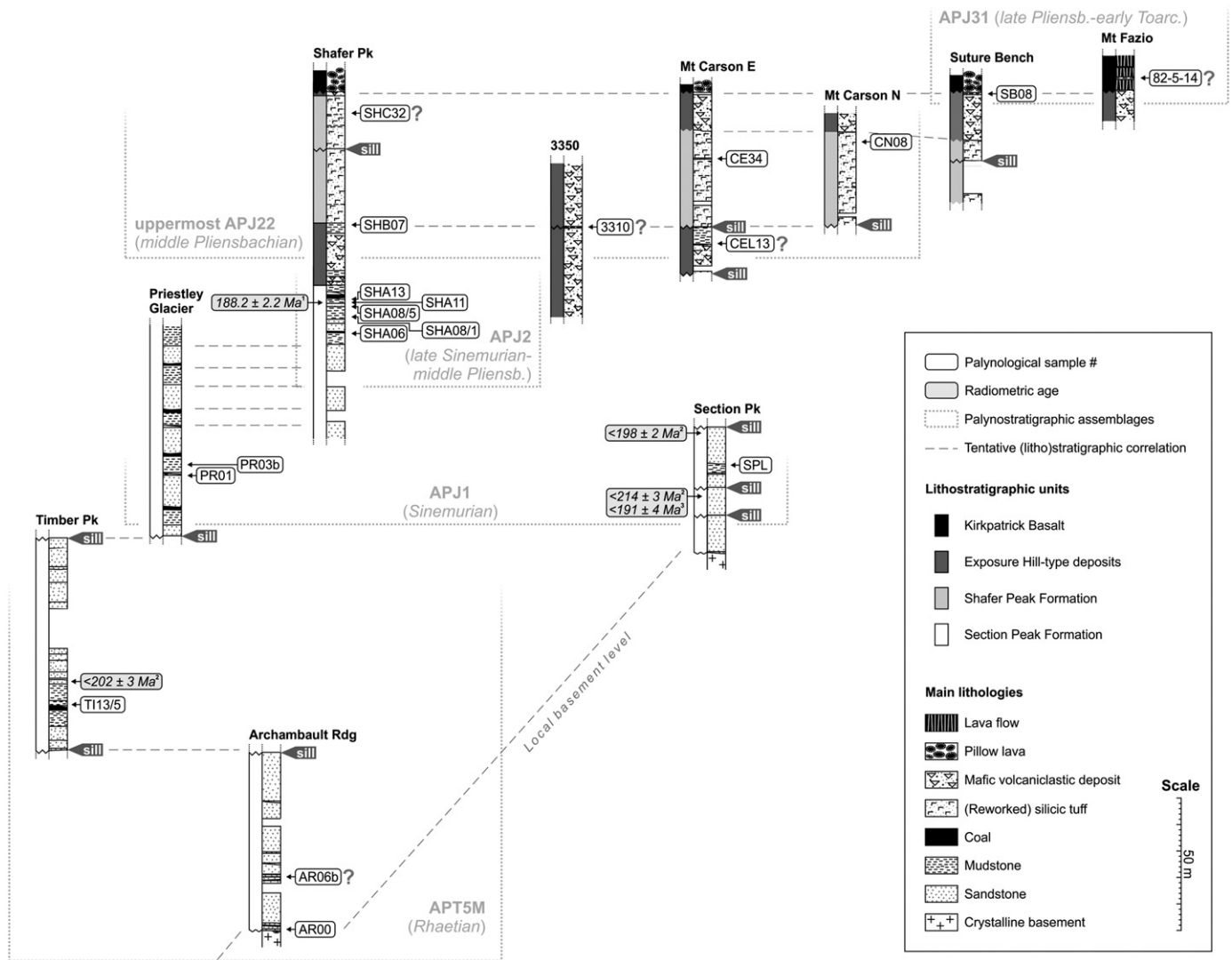


Fig. 2. Inferred litho- and palynostratigraphic correlation of the studied sedimentary sections in southern north Victoria Land, East Antarctica.

Radiometric ages after Elsner (2010)¹, Elsner et al. (2013)², and Goodge and Fanning (2010)³ [the former is a U–Pb (SHRIMP) age from juvenile zircon in a tuff-rich layer; the latter two represent maximum-age constraints based on detrital-zircon ages].

Fig. 7.2) are followed in this work. Further, for the Late Triassic, Price (1997: Fig. 7), although recognising the Carnian and Norian, did not distinguish the Rhaetian, apparently including it in the latter (presumably following some previous authors who had regarded the Rhaetian as an equivalent of the upper part of the Norian; e.g., Tozer, 1988). This view has not been substantiated by the International Commission on Stratigraphy, as, for example, in their recent printed version (as well as previous versions) of the International Chronostratigraphic Chart (Gradstein et al., 2012; <http://www.stratigraphy.org/index.php/ics-chart-timescale>).

Moreover, Price's (1997) subdivision of his palynological unit APT5 [in the lower Bundamba Group (Clarence–Moreton Basin)], which spans the latest Triassic–earliest Jurassic, is not followed, because the stratigraphic order of species used (in eastern Australia) to achieve second- and third-order zonation cannot be upheld. This view is based on current knowledge of miospore distribution in the continental strata of the lower Bundamba Group and equivalent marine rocks of the New Zealand succession, which have been accurately dated by ammonites (de Jersey and Raine, 1990; Stevens, 2004; de Jersey and McKellar, 2013; N.J. de Jersey, personal communication, 2013).

The first appearance of *Polycingulatisporites crenulatus* and the level of introduction of abundant to dominant *Classopollis* (*Corollina torosa*

as employed by Price, 1997) define respectively the base and, essentially, the upper limit of APT5 (the latter representing the coincident base of his succeeding unit, APJ1). Other species, the appearances of which Price used in subdivision of APT5, embrace (in the ascending stratigraphic order ascribed to them by that author) *Polycingulatisporites mooniensis*, *Retitriletes rosewoodensis*, *Craterisporites rotundus* (last appearance), *Zebrasporites interscriptus*, *Anapiculatisporites* (*Ceratisporites*) *helidonensis*, and *Retitriletes austroclavatoides*. Of these, *P. mooniensis* is rare and sporadically distributed in the lower limit of its range, as is *R. rosewoodensis*, which, in the New Zealand succession, is known to extend down to the Warepan (mid–upper Norian), while both *P. crenulatus* and *P. mooniensis* have been recorded there from as low as the Otamitan [mid-Norian; de Jersey and Raine (1990); also, for the relationship between the New Zealand Otamitan Stage and the international Norian Stage, see Raine et al. (2012) for recalibration of the New Zealand Geological Timescale against the International Geological Timescale of Gradstein et al. (2012)]. In south-eastern Queensland, the latter two species (*P. crenulatus* and *P. mooniensis*) appear in the Rhaetian, at the base of the Clarence–Moreton Basin and the Bundamba Group therein (see below). On the other hand, *Perinopollenites elatoides* is not known to occur below the Rhaetian of south-eastern Queensland and the Otapirian (Rhaetian)

of New Zealand (de Jersey and Raine, 1990: p. 55, figure 4.4). *Anapiculatisporites helidonensis* appears in the Rhaetian of the basal Bundamba Group (Raceview Formation) and equivalents (e.g., de Jersey, 1971; McKellar, 1985), but has not been reported from New Zealand. The important index *Z. interscriptus*, in the eastern Clarence–Moreton Basin, has been documented from the lower Hettangian (lower Ripley Road Sandstone) and, in New Zealand, from the Aratauran (Hettangian and lowermost Sinemurian) (Zhang and Grant-Mackie, 2001; de Jersey and Raine, 1990; de Jersey and McKellar, 2013; N.J. de Jersey, personal communication, 2013).

Retitrites austroclavatoides, which Price (1997) used to define the base of his third-order subunit, APT522, appears at, or immediately above, the Triassic–Jurassic (Rhaetian–Hettangian) boundary in New Zealand (de Jersey and Raine, 1990; de Jersey and McKellar, 2013; compare Zhang and Grant-Mackie, 2001). In the eastern Clarence–Moreton Basin, it has been reported a little above the System boundary, in the lowermost Ripley Road Sandstone (de Jersey and McKellar, 2013). However, because of the paucity of suitable material in this sandstone-dominated succession, the species may extend to the base of the formation and also mark the Triassic–Jurassic boundary there. Further delineating the boundary in both New Zealand and eastern Australia is the incoming of *Toripustulatisporites hokonuiensis* de Jersey, a species applied in definition of the Hettangian–earliest Sinemurian *T. hokonuiensis* Association Zone (de Jersey and McKellar, 2013).

For interpretation of the present work and based largely on species ranges given by de Jersey and Raine (1990) and de Jersey and McKellar (2013) for New Zealand and eastern Australia, outlined above, APT5 is here subdivided into *Lower*, *Middle*, and *Upper* subzones (APT5L, APT5M, APT5U) (Fig. 3), the base of the latter two being defined respectively by the appearances of *Foveosporites moretonensis* and *Toripustulatisporites hokonuiensis*. In use of *Lower*, *Middle*, and *Upper* subdivisions, the alphanumeric systematization used by Price (1997), and previously by Price et al. (1985), is not strictly followed, in order to avoid confusion and thus clearly differentiate these new subunits from those defined previously by Price and colleagues.

Further, the formal zonations for the Late Triassic–Early Jurassic of New Zealand (de Jersey and Raine, 1990) and Australia (de Jersey and

McKellar, 2013) are amalgamated to provide a standardised zonation for both of these eastern Gondwanan regions. In so doing, alignment has been achieved between the informal and formal schemes. However, the informal scheme has been employed in the current study, as the formal equivalent, for the post-Hettangian Lower Jurassic, is in need of further subdivision. Despite this, it is not proposed that application of the modified informal zonal subdivision be extended into the New Zealand region. The informal–formal zonal alignment, for the attendant part of the stratigraphic section in question, has been provided here primarily to highlight relationships.

4.1.1. Modification of the informal alphanumeric zonation of APT5 (Price, 1997) (Fig. 3)

Three new informal alphanumeric subdivisions of APT5 (Price, 1997) are proposed. As outlined above, the biostratigraphic integrity of Price's subunits of APT5 cannot be sustained in the lower Bundamba Group of eastern Australia. A further issue with the alphanumeric subdivision of this zone, and the like, is that the alphanumeric code cannot readily be adapted, without causing even greater confusion, to changes in the stratigraphic location of system boundaries. This is the case here with placement of the Triassic–Jurassic (Rhaetian–Hettangian) Boundary at the base of APT5U [such that the division (as defined biostratigraphically by Price, 1997) between APT5 and the succeeding unit, APJ1, occurs in the lower Sinemurian, somewhat above the base of the Jurassic (with “T” and “J” representing the Triassic and Jurassic respectively)].

4.1.1.1. Lower APT5 (APT5L) – new subzone. Apart from embracing *Polycingulatisporites crenulatus* and *Polycingulatisporites mooniensis*, the new subunit APT5L includes *Craterisporites rotundus* [which appears in older Late Triassic (Carnian) strata of south-eastern Queensland (*Craterisporites rotundus* Zone of de Jersey, 1975; see Helby et al., 1987) and in the late Middle Triassic of New Zealand] and embraces, within the zone, the first appearance of *Retitrites rosewoodensis* (Fig. 3). This unit equates in the New Zealand succession with the *P. crenulatus* Zone of de Jersey and Raine (1990), marked at its upper limit by the appearance of *Foveosporites*

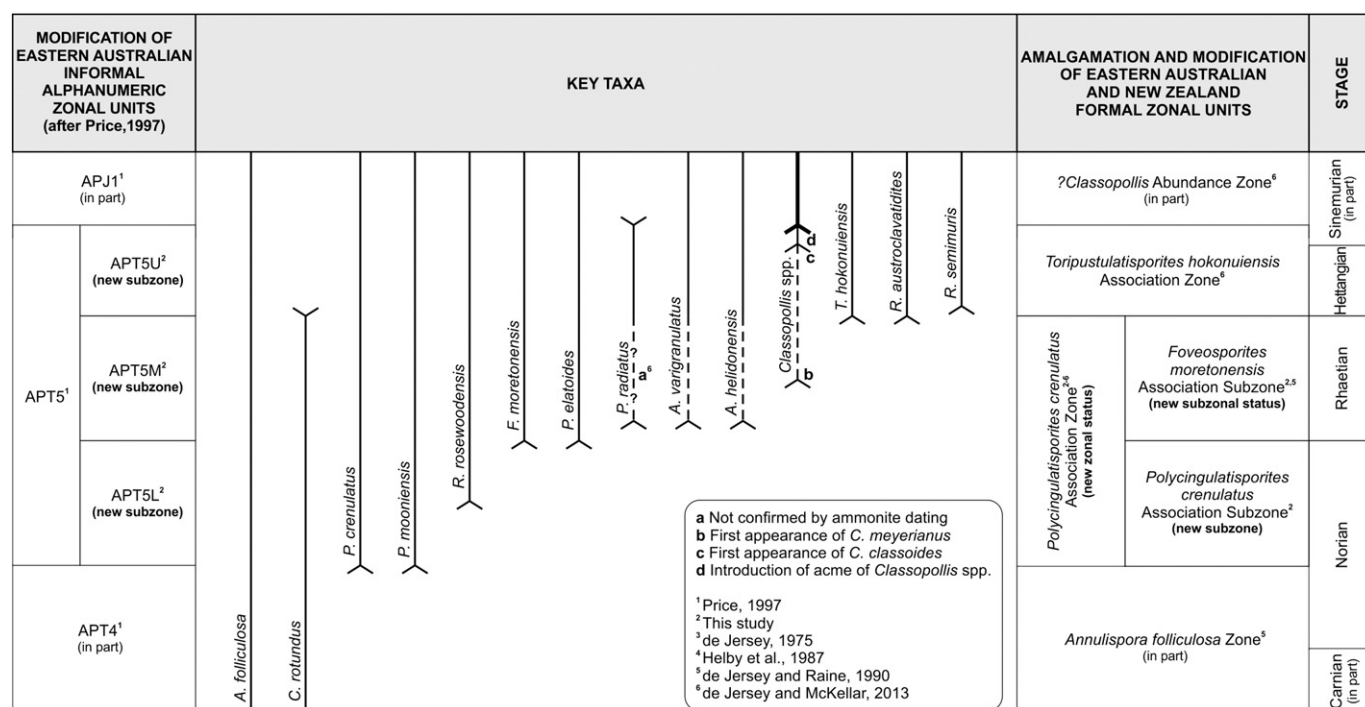


Fig. 3. Subdivision of unit APT5 into lower (APT5L), middle (APT5M) and upper (APT5U) subzones proposed herein, with ranges of key taxa, inferred ages, and correlation with a combined and modified formal palynostratigraphic zonation for eastern Australia and New Zealand.

moretonensis, the latter incoming applied by the cited authors in definition of their *F. moretonensis* Zone (Fig. 4) (note that the *crenulatus* and *moretonensis* zones of de Jersey and Raine are combined below to form the *P. crenulatus* Association Zone, embracing a lower *P. crenulatus* Association Subzone and an upper *F. moretonensis* Association Subzone).

de Jersey and Raine (1990, p. 61, Fig. 4.3) assigned a (late) “Early to Late Norian” (essentially middle to late Norian) age to their *Polycingulatisporites crenulatus* Zone, which, although present in New Zealand, is absent (as defined by them for New Zealand) from eastern Australia due to mid–late Norian hiatus (below the base of the Bundamba Group); this resulted from widespread tectonism (e.g., Jell, 2013) which terminated the early Late Triassic (Carnian–early Norian) Ipswich Coal Measures and equivalents (encompassed by the *Craterisporites rotundus* Zone; e.g., de Jersey, 1975; de Jersey and Raine, 1990: Fig. 4.4; N.J. de Jersey, personal communication, 2013). Similarly, the new subunit APT5L is not recorded in the present study of NVL, but palynofloras from the lower Falla Formation (Farabee et al., 1989, 1990) in the CTM, in containing the association of *P. crenulatus* and *C. rotundus*, are seemingly conformable with this subzone; the exact provenance of the only sample containing *P. crenulatus*

in the Falla Formation, however, is unknown (Farabee et al., 1989: Fig. 1 and Table 1).

4.1.1.2. Middle APT5 (APT5M) — new subzone. APT5M is defined by the incoming of *Foveosporites moretonensis* at its lower limit and of *Toripustulatisporites hokonuiensis* at its upper limit. The subzone includes the first appearances of *Perinopollenites elatoides* and rare *Anapiculatisporites helidonensis* and *Antulsporites varigranulatus* (Fig. 3); the oldest Queensland record of the latter species, referred to as *Antulsporites* sp. A, is from strata dated as Rhaetian in the north-western Surat Basin by McKellar (1978, personal observation). APT5M essentially equates with the *F. moretonensis* Zone of de Jersey and Raine (1990), which was instituted by these authors in the New Zealand succession and dated by them as Otapirian (Rhaetian). However, de Jersey and Raine's *moretonensis* Zone was defined at its upper limit by the incoming of *Retitriletes austroclavatidites*, which first occurs at about the same level as *T. hokonuiensis*, at the Triassic–Jurassic boundary, in both New Zealand and eastern Australia (de Jersey and McKellar, 2013). Further, de Jersey and Raine's zone is amended in status below and referred to as the *F. moretonensis* Association Subzone of a newly redefined *Polycingulatisporites crenulatus* Association Zone (modified

SERIES	STAGE	EASTERN AUSTRALIA					NEW ZEALAND	MODIFIED SCHEME FOR EASTERN AUSTRALIAN AND NEW ZEALAND ZONAL UNITS (this study; modifications in bold)					
		de Jersey, 1975 (in part)	de Jersey, 1976	Helby et al., 1987 (in part)	Price, 1997 (in part)	de Jersey and McKellar, 2013	de Jersey and Raine, 1990, 2002 (in part)	Informal Units (after Price, 1997)	Formal Units (after cited authors)				
LOWER JURASSIC	Toarcian			<i>Callialasporites turbatus</i> “Oppel” Zone (in part)	APJ3 (in part)			APJ3 (in part)	<i>?Classopollis</i> Abundance Zone (strata with common <i>Classopollis</i> : de Jersey and McKellar, 2013, p.27; N.J. de Jersey, pers. comm., 2014)				
	Pliensbachian		Assemblage D	<i>Corollina torosa</i> “Oppel” Zone		APJ2	APJ22			<i>Retitriletes austroclavatidites</i> Zone (= Assemblages III and IV of Zhang and Grant-Mackie, 2001; Assemblage III = <i>T. hokonuiensis</i> Assoc. Subzone)	APJ2	APJ22	
	Sinemurian	<i>Trisaccites variabilis</i> Zone			APJ21			APJ12					APJ11
	Hettangian	<i>Polycingulatisporites crenulatus</i> Zone	Assemblage B			<i>Toripustulatisporites hokonuiensis</i> Association Zone		APT5U		<i>Toripustulatisporites hokonuiensis</i> Association Zone			
Rhaetian		Assemblage A		<i>Polycingulatisporites crenulatus</i> “Oppel” Zone	APT5 (Price’s subdivision unworkable in eastern Australia)	<i>Polycingulatisporites crenulatus</i> Zone	<i>Foveosporites moretonensis</i> Zone (= Assemblage II of Zhang and Grant-Mackie, 2001) <i>Polycingulatisporites crenulatus</i> Zone (= Assemblage I of Zhang and Grant-Mackie, 2001)	APT5M	<i>Foveosporites moretonensis</i> Association Subzone				
UPPER TRIASSIC	Norian	hiatus						APT5L	<i>P. crenulatus</i> Association Subzone				
	Carnian	<i>Craterisporites rotundus</i> Zone		<i>Craterisporites rotundus</i> “Oppel” Zone	APT4 (in part – extends down into latest Middle Triassic)		<i>Annulispora folliculosa</i> Zone (in part – extends down into latest Middle Triassic)	APT4 (in part – extends down into latest Middle Triassic)	<i>Annulispora folliculosa</i> Zone (in part – extends down into latest Middle Triassic)				

Fig. 4. Relationships between the various zonal schemes for eastern Australia and New Zealand, and the zonal-scheme amendments (in bold) proposed in the present study. Note that (1) zonal relationships have been given pre-eminence over the ages (here updated) that were originally assigned to the zonal units by the instituting/cited authors; (2) the scheme of Reiser and Williams (1969), for the Surat Basin in eastern Australia, has been omitted; and that (3) the New Zealand *Annulispora folliculosa* Zone of de Jersey and Raine (1990; = APT4 of Price, 1990) is preferably applied to the essentially equivalent section in eastern Australia in lieu of the *Craterisporites rotundus* Zone, as *C. rotundus* is rare in New Zealand, with *A. folliculosa* thus being the favoured index for both regions (N.J. de Jersey, personal communication, 2014).

Sample	AR 00	AR 06b	TI 13/5	SPL	PR 01	PR 03b	SHA 06	SHA 08/1	SHA 08/5	SHA 11	SHA 13	33 10	CEL 13	SHB 07	CE 34	CN 08	SHC 32	SB 00	82-5 -14
Palynomorph yield	R	L	R	M	L	M	R	R	R	R	R	L	L	R	R	M	L	R	L
Palynomorph preservation	G	P	G	F	F	F	F	F	G	E	G	F	P	E	G	F	M	G	M
Lithostratigraphic unit	Section Peak Formation											low. EH-type deposits			Shafer Peak Fm.			u. EHT	Kirkp.
<i>Alisporites</i> spp. (indet.)	•	•	•	•	•	•	•	•	•	•	•	•	•	•	•	•	•	•	•
<i>Anapiculatisporites cooksonae</i>	•							•	•	•	•								
<i>Anapiculatisporites pristidentatus</i>	•							•			•								
<i>Annulispora</i> spp. (indet.)	•		•							•			•	•				•	•
<i>Antulsporites varigranulatus</i>	•		•	•				•		•	•			•					•
<i>Antulsporites</i> spp. (indet.)	•									•	•			•					
<i>Aratrisporites</i> spp.	•		•						•										
<i>Cadargasporites baculatus</i>	•																		
<i>Cadargasporites cuyanensis</i>	•																		
<i>Cadargasporites granulatus</i>	•						•		•			•			•	•	•		
<i>Cadargasporites reticulatus</i>	•						•								•		•		
<i>Cadargasporites senectus</i>	•																		
<i>Cibotiumspora</i> spp.	•			•			•		•	•		•		•	•	•		•	
<i>Converrucosisporites cameronii</i>	•		•					•	•	•	•			•					
<i>Craterisporites rotundus</i>	•		•																
<i>Cyathidites minor</i> (Delto. directa)	•		•	•			•	•	•	•	•		•	•	•	•		•	•
<i>Cyathidites australis</i>	•		•	•			•	•	•	•	•		•					•	
<i>Cycadopites</i> spp. (indet.)	•		•	•	•				•	•	•		•	•	•	•		•	
<i>Dictyophyllidites</i> spp.	•	•	•					•	•	•	•	•		•	•	•		•	•
cf. <i>Dijkstrastrisporites</i> sp.	•									•	•								
<i>Foveosporites moretonensis</i>	•								•	•	•			•					
cf. <i>Granuloperculatispollis</i> sp.	•																		
<i>Inaperturopollenites</i> spp.	•		•	•		•	•		•						•	•	•	•	
<i>Limbosporites</i> spp.	•		•																
cf. <i>Lundbladispota</i> sp.	•																		
<i>Marattisporites scabratus</i>	•		•				•				•	•							
<i>Megamonoporites</i> sp.	•																		
<i>Neoraistrickia</i> spp.	•		•				•	•	•	•				•				•	
<i>Nevesisporites vallatus</i>	•																		
<i>Osmundacidites wellmanii</i>	•		•		•	•	•	•	•		•	•		•	•	•		•	•
<i>Platysaccus queenslandii</i>	•		•	•				•			•								
<i>Polycingulatisporites crenulatus</i>	•		•							•									
<i>Polycingulatisporites radiatus</i>	•																		
<i>Polycingulatisporites</i> sp.	•							•		•				•					
<i>Punctatosporites walkomii</i>	•							•						•					
<i>Rogalskaisporites</i> spp.	•		•				•	•		•				•					
<i>Schizosporis scissus</i>	•		•																
<i>Stereisporites</i> spp.	•		•				•	•	•	•	•		•	•		•			
<i>Sulcatisporites institatus</i>	•		•																
<i>Thymospora ipsviciensis</i>	•		•					•				•		•					
<i>Todisporites minor</i>	•		•					•						•	•				
cf. <i>Triplexisporites playfordii</i>	•																		
<i>Tuberculatosporites aberdarensis</i>	•		•									•							
<i>Uvaesporites</i> spp.	•		•		•		•		•	•	•	•			•	•		•	
<i>Verrucosisporites varians</i>	•		•					•	•	•		•						•	
cf. <i>Ashmoripollis reducta</i>		•											•						
<i>Apiculatisporites globosus</i>			•						•	•				•					
Palynostratigraphic assemblage type	APT5M				APJ1			APJ2					uppermost APJ22					APJ31	
Inferred age	Rhaetian				Sinemurian			late Sinemurian - middle Pliensb.					middle Pliensbachian					late Pliensb.-early Toarcian	

Fig. 5. Collection number, yield (L = low; M = moderate; R = rich), preservation (P = poor; F = fair; G = good; E = excellent), stratigraphic occurrence, palynomorph content, and inferred age of productive samples from the Triassic–Jurassic succession in southern north Victoria Land, East Antarctica.

Sample	AR 00	AR 06b	AR 13/5	TI	SPL	PR 01	PR 03b	PR	SHA 06	SHA 08/1	SHA 08/5	SHA 11	SHA 13	SHA 13	33 10	CEL 13	SHB 07	CE 34	CN 08	SHC 32	SB 00	82-5 -14
Palynomorph yield	R	L	R	G	M	L	M		R	R	R	R	R	R	L	L	R	R	M	L	R	L
Palynomorph preservation	G	P	G		F	F	F		F	F	G	E	G	G	F	P	E	G	F	M	G	M
Lithostratigraphic unit	Section Peak Formation																					
<i>Araucariacites</i> spp.	•		•		•	•	•			•	•					•	•	•	•	•	•	•
<i>Baculatisporites comauensis</i>	•		•		•	•	•		•	•	•	•					•				•	
<i>Calamospora tener</i>	•		•		•		•		•	•							•					
<i>Circulispores parvus</i>	•		•																			
<i>Concavisporites</i> sp.	•																					
<i>Densosporites</i> spp. (indet.)	•				•				•	•	•	•			•	•	•	•			•	•
<i>Indusiisporites parvisaccatus</i>	•									•		•	•		•	•		•				
<i>Laevigatosporites ovalis</i>	•																					
<i>Lycospora pallida</i>	•																					
<i>Pityosporites antarcticus</i>	•				•				•	•	•	•	•			•		•				
<i>Prototraploxypinus samolovichii</i>	•																					
<i>Rugulatisporites</i> spp.	•								•										•			
<i>Sulcosaccispora lata</i>	•								•													
<i>Vitreisporites pallidus</i>	•								•	•	•	•	•		•	•	•	•	•	•	•	•
<i>Classopolis</i> spp.					•				•	•	•	•			•	•		•				
<i>Anapiculatisporites helidonensis</i>					•																	
cf. <i>Exesipollenites tumulus</i>					?				•	•	•	•	•		•		•					
<i>Retiriletes austroclavatoides</i>					?		•		•	•	•	•	•		•		•				•	
<i>Retiriletes rosewoodensis</i>									•	•	•	•					•					
<i>Trachysporites infirmus</i>					•												•				•	•
<i>Perinopollenites elatoides</i>																						
<i>Striatella seebergensis</i>					•		?											•	•		•	•
<i>Granulatisporites minor</i>									•	•	•	•	•		•		•					
<i>Ischyosporites punctatus</i>									•	•	•	•	•		•		•					
<i>Podosporites variabilis</i>									•	•	•	•	•				•					?
<i>Retiriletes semiminuris</i>										•	•	•	•		•		•				•	
<i>Podocarpidites</i> spp. (indet.)									•	•	•	•	•		•		•				•	
<i>Nevesisporites</i> sp.										•	•	•	•				•				•	

Fig. 5 (continued).

from: de Jersey, 1975; Helby et al., 1987; de Jersey and Raine, 1990; de Jersey and McKellar, 2013) (Figs. 3, 4).

Miospore assemblages reported here from NVL are ascribed to APT5M. In eastern Australia, palynofloras from the upper Callide Coal Measures (central-eastern Queensland), which were referred to by Farabee et al. (1989) in their above-cited study of the Falla Formation, are probably conformable with this subzone, as they contain *Foveosporites moretonensis* and *Polycingulatisporites crenulatus*, and lack both *Retitriteles austroclavatidites* and abundant *Classopollis* (*Corollina*) (de Jersey, 1974; Stevens, 1981: Text-fig. 6). This favours Stevens' "correlation alternative 1", which points to Norian hiatus between the lower Callide Coal Measures (*Craterisporites rotundus* Zone) and the upper Callide Coal Measures [*P. crenulatus* Zone of de Jersey (1975; as cited and modified in age by Stevens) attributed below, with formal zonal amendments, to the *F. moretonensis* Association Subzone of the *P. crenulatus* Association Zone; Fig. 4]. The upper measures are thus regarded as being correlative with the (Rhaetian) basal Bundamba Group in the Clarence–Moreton Basin, despite the absence of several species typical of this part of the section (N.J. de Jersey, personal communication, 2013).

4.1.1.3. Upper APT5 (APT5U) – new subzone. Extending from the appearance of *Toripustulatisporites hokonuiensis*, at about the base of the Jurassic, to the incoming of abundant *Classopollis*, APT5U is equivalent to the Hettangian–earliest Sinemurian *T. hokonuiensis* Association Zone of de Jersey and McKellar (2013) in the lower Bundamba Group (lower Ripley Road Sandstone). It is also essentially equivalent to APT522 of Price (1997; defined at its base by the appearance of *Retitriteles austroclavatidites*), and the lower part of the *R. austroclavatidites* Zone of de Jersey and Raine (1990, 2002), the latter instituted in New Zealand (Fig. 4).

Price has stated that cheirolepidiacean pollen are "[...] established at the base of Unit APJ1 (i.e., marking the upper limit of APT5), with the strongly infra-rugulate to striate variety of *Corollina torosa* making its appearance" (Price, 1997: p. 168). According to de Jersey and McKellar (2013), intrastriate *Classopollis*, recorded by them as *Classopollis* sp. cf. *Classopollis chateauvovi* (equivalent to *Corollina torosa*/*Classopollis torosus* and *Classopollis classoides* of other authors), although becoming abundant in south-eastern Queensland and New Zealand in the early, post-basal Sinemurian, first appears only marginally lower in the succession about the Hettangian–Sinemurian boundary, based on stratigraphic relationships established with the ammonite dating of Stevens (2004) in the New Zealand region (also see below). The acme of *Classopollis* has been referred to as the Cheirolepidiacean Phase by Balme (2000).

APT5U has not been reported in the present study of assemblages from NVL. In south-eastern Queensland, strata embraced by the equivalent *Toripustulatisporites hokonuiensis* Zone are almost entirely confined to a rarely preserved succession of Hettangian deposits in the lower

Bundamba Group of the eastern Clarence–Moreton Basin (Logan Sub-basin, east of the major structure of the West Ipswich Fault) and adjacent coastal Nambour Basin of south-eastern Queensland (de Jersey and McKellar, 2013). The continental succession in this part of the Bundamba Group in these two basins, primarily that in the eastern Clarence–Moreton Basin, has been correlated palynologically (de Jersey and McKellar, 2013) with a complete, accurately dated boundary sequence in New Zealand (see Stevens, 2004). Global unconformity generally consumes the Triassic–Jurassic Boundary: the Hettangian is missing from most onshore areas of Australia and only a handful of localities are presently known world-wide where the succession across the System boundary is complete, including one in the southern part of South Island, New Zealand (Stevens, 2004; de Jersey and McKellar, 2013).

APT5 palynofloras are generally further characterized by abundant *Alsiporites* spp., although, in New Zealand, there is a marked decline of these pollen in the early Hettangian (early Aratauran, i.e., in APT5U equivalents), contrasting with the Hettangian of south-eastern Queensland, where there is a more gradual decline (de Jersey and Raine, 1990; de Jersey and McKellar, 2013). Another taxon of significance is *Polycingulatisporites radiatus* Zhang and Grant-Mackie 1997 (= *Polycingulatisporites* sp. cf. *Polycingulatisporites mooniensis* of de Jersey and Raine, 1990). This species was reported by Zhang and Grant-Mackie (2001) from the Otapirian (Rhaetian) and Aratauran (Hettangian–early Sinemurian) of New Zealand, although, according to de Jersey and McKellar (2013), the precise age of the Otapirian records is in need of confirmation. In the present work, this species has been documented in an APT5M (Rhaetian) palynoflora.

4.1.2. Amalgamation and modification of New Zealand and eastern Australian formal zonal units (Fig. 4)

Paralleling the above modifications to Price's (1997) informal alphanumeric zonation, the equivalent formally defined palynostratigraphic zones for the eastern Australian and New Zealand regions are integrated here, to establish a biostratigraphic subdivision that can be applied to both regions, which have different parts of the associated stratigraphic section variously preserved.

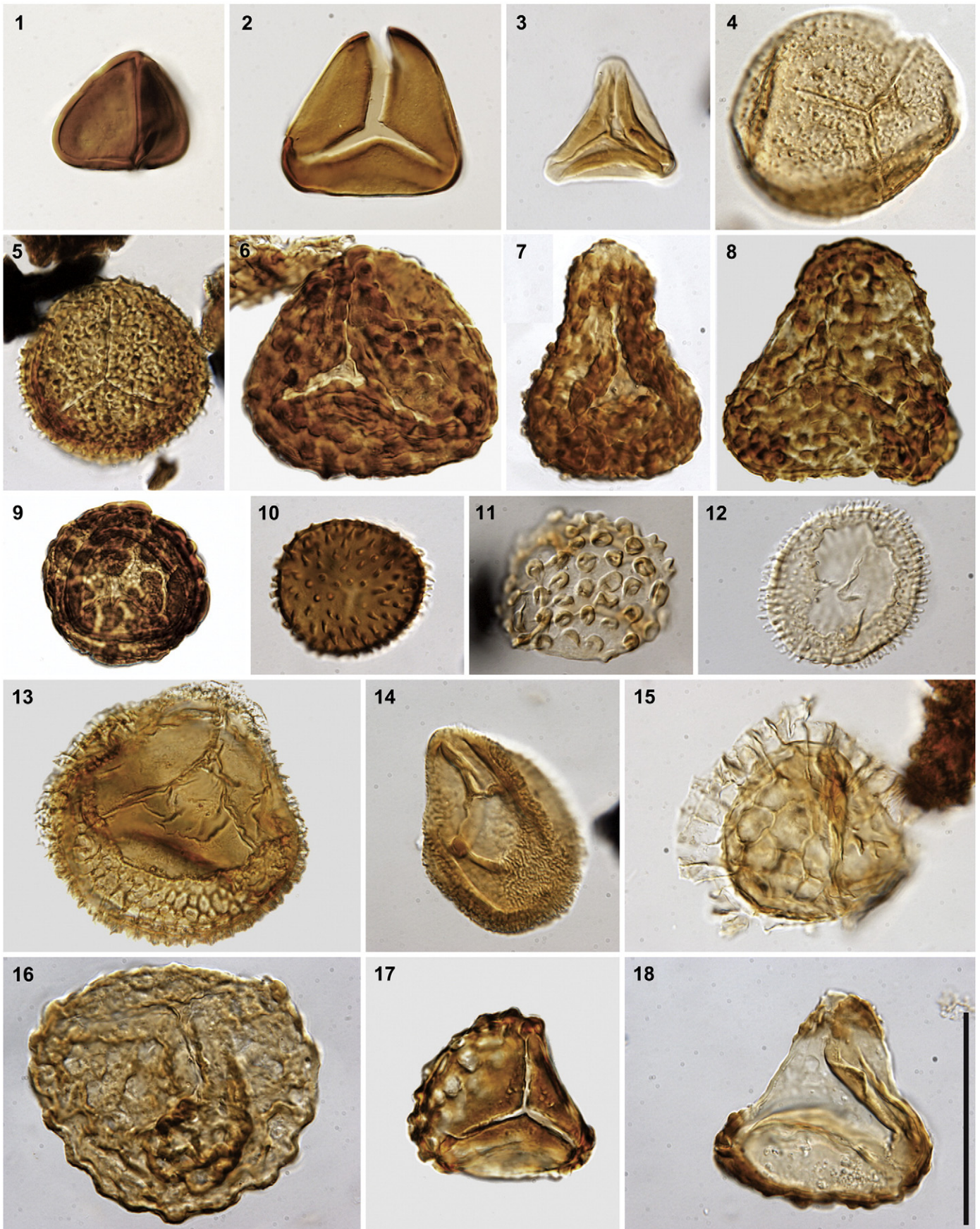
4.1.2.1. *Polycingulatisporites crenulatus* Association Zone (de Jersey, 1975; Helby et al., 1987; de Jersey and Raine, 1990; de Jersey and McKellar, 2013) – new zonal status.

The *crenulatus* Zone, as indicated by the references in Fig. 4, has been subjected to ongoing redefinition and application since its initial establishment by de Jersey (1975).

Here, the recent concepts of the zone, as applied differently in New Zealand (de Jersey and Raine, 1990) and eastern Australia (Helby et al., 1987; de Jersey and McKellar, 2013), are taken into a united framework. In order to achieve this, the Otapirian (Rhaetian) *Foveosporites moretonensis* Zone of de Jersey and Raine (1990) has been changed in status to an association subzone that represents the upper of two association subzones encompassed by a newly redefined

Plate I. Composite micrographs of selected spore taxa from the Upper Triassic and Lower Jurassic of north Victoria Land, East Antarctica, with sample and slide number and England Finder coordinates. Scale bar = 50 µm.

- 1: *Cyathidites minor* Couper; GIX-SHA11-1; M26/2.
- 2: *Cyathidites australis* Couper; GIX-SHA11-2; C50/2.
- 3: *Dictyophyllidites mertonii* (de Jersey) Playford et Dettmann; GIX-AR00-4; F38/4.
- 4: *Osmundacidites wellmanii* Couper; GIX-SHA08/5-4; H44/0.
- 5: *Baculatisporites comamensis* (Cookson) Potonié; GIX-SHA08/1-1; Q28/3.
- 6–8: cf. *Concavissimisporites-Impardecispora* sp. indet.; (6) GIX-SB08n-1; P52/4. (7) GIX-SB08-6; C24/0. (8) GIX-SB08n-2; J46/3.
- 9: *Uvaesporites verrucosus* (de Jersey) Helby; GIX-TI13/5-2; F53/0.
- 10: *Anapiculatisporites helidonensis* (de Jersey) de Jersey et McKellar; GIX-SPL-6; J37/0.
- 11: *Craterisporites rotundus* de Jersey; GIX-AR00-5; U44/4.
- 12: *Cadargosporites baculatus* de Jersey et Paten emend Reiser and Williams; GIX-AR00-5; G41/4.
- 13: *Cadargosporites reticulatus* de Jersey et Paten; GIX-CE34-1; M45/4.
- 14: *Cadargosporites senectus* de Jersey et Hamilton; GIX-AR00-4; L40/2.
- 15: *Retitriteles austroclavatidites* (Cookson) Döring, Krutzsch, Mai et Schulz; GIX-SHA08-5-2; R32/1.
- 16: *Klukisporites variegatus* Couper; GIX-SB08-6; R42/0.
- 17: *Ischyosporites punctatus* Cookson et Dettmann; GIX-CE34-1; M31/0.
- 18: cf. *Trilobosporites antiquus* Reiser et Williams; GIX-SB08-6; D39/1.



Polycingulatisporites crenulatus Association Zone. The upper boundary of de Jersey and Raine's zone has also been redefined.

The *crenulatus* Association Zone equates with the new informal sub-units APT5L and APT5M (Fig. 4; see Sections 4.1.1.1 and 4.1.1.2) in the attendant complement of appearing species (Fig. 3). It is succeeded by the Hettangian–earliest Sinemurian *Toripustulatisporites hokonuiensis* Association Zone (de Jersey and McKellar, 2013; = APT5U), based on the first appearance of its nominate species at the Rhaetian–Hettangian (Triassic–Jurassic) boundary.

4.1.2.2. *Polycingulatisporites crenulatus* Association Subzone — new subzone. The *Polycingulatisporites crenulatus* Association Subzone (middle–late Norian) is equivalent to APT5L (Fig. 4), delimited at its lower and upper limits respectively by *P. crenulatus* and *Foveosporites moretonensis*. First appearing in the zone are *Polycingulatisporites mooniensis* and *Retitriteles rosewoodensis* (Fig. 3).

This association subzone, which has been reported in New Zealand as the equivalent (and here displaced) *Polycingulatisporites crenulatus* Zone (de Jersey and Raine, 1990), is not presently known to occur in eastern Australia because of hiatus at the base of the Bundamba Group (e.g., Jell, 2013).

4.1.2.3. *Foveosporites moretonensis* Association Subzone — new subzone. The *Foveosporites moretonensis* Association Subzone (Rhaetian) equates with APT5M. Strata previously embraced by the superseded *Polycingulatisporites crenulatus* Zone [sensu de Jersey and McKellar (2013): essentially the Aberdare Conglomerate and Raceview Formation, basal Bundamba Group] in southeastern Queensland can be associated with this association subzone, together with the upper part of the Callide Coal Measures, discussed above.

The first appearances of *Foveosporites moretonensis* and *Toripustulatisporites hokonuiensis* (the latter species being unreported in the current study) are used to delineate the lower and upper boundaries of the *F. moretonensis* Association Subzone. *Retitriteles austroclavitudites*, as indicated above, can be used as a proxy for the association subzone's upper limit, effectively the Triassic–Jurassic boundary.

Species first appearing in the *Foveosporites moretonensis* Association Subzone include *Perinopollenites elatoides*, *Anapiculatisporites helidonensis* and *Antulsporites varigranulatus* (Fig. 3).

4.2. Implications for extrapolation of the palynostratigraphy of eastern Australia to NVL

The presence of two major unconformities (mid–late Norian and Hettangian to possibly earliest Sinemurian), related to tectonism in

the Late Triassic and Early Jurassic of eastern Gondwana, and the above-outlined complexities of biostratigraphic interpretation of, and correlation in, this part of the section have implications for comprehension of the palynostratigraphy and the completeness of the stratigraphic succession of NVL, considering the limited thickness of its Late Triassic–Early Jurassic succession.

5. Palynostratigraphic assessment and dating of NVL assemblages

In terms of Price's (1997) palynostratigraphic scheme with the modifications described above, five assemblage types have been recognised in the studied samples from the Upper Triassic and Lower Jurassic of NVL (Fig. 2): (1) APT5M assemblages in the basal and middle part of the Section Peak Formation; (2) APJ1 assemblages in the upper part of the Section Peak Formation, excluding its uppermost strata; (3) APJ2 assemblages in the uppermost part of the Section Peak Formation; (4) uppermost APJ22 assemblages in the lower Exposure Hill-type deposits and the Shafer Peak Formation; and (5) APJ31 assemblages in the upper Exposure Hill-type deposits and Kirkpatrick Basalt interbeds.

5.1. APT5M assemblages (Rhaetian)

Stratigraphic occurrence (Fig. 2): Basal part of the Section Peak Formation at Archambault Ridge (samples AR00 and AR06b); middle part of the Section Peak Formation at Timber Peak (sample TI13/5).

Description: Two samples from the base (AR00) and from the middle part (TI13/5) of the Section Peak Formation have yielded very rich and diverse palynological assemblages (Fig. 5). They are characterized by a high abundance of *Alisporites australis* (>30%) and the joint occurrences of the stratigraphically significant taxa *Craterisporites rotundus* (Plate I, 11), *Polycingulatisporites crenulatus* (Plate II, 10), and *Antulsporites varigranulatus* (Plate II, 8). The assemblages are further distinguished by a high diversity of monolete spores [e.g., *Thymospora ipsviciensis* (Plate II, 19), *Tuberculatosporites aberdarensis* (Plate II, 20), *Aratrisporites* spp. (Plate II, 21)] and bryophytic spores [e.g., *Annulispora* spp. (Plate II, 1, 2), *Rogalskaisporites cicatricosus* (Plate II, 3), and *Stereisporites* spp. (Plate II, 5, 6)]. Sample AR00 also contains *Foveosporites moretonensis* (Plate II, 4), *Polycingulatisporites radiatus* (Plate II, 9) and a high diversity of *Cadargasporites*, including *Cadargasporites reticulatus* (Plate I, 13).

Sample AR06b from ca 20 m up-section at Archambault Ridge yielded a few poorly preserved palynomorphs, including *Alisporites australis*, *Alisporites lowoodensis* (Plate III, 5), *Dictyophyllidites mortonii*

Plate II. Composite micrographs of selected spore taxa from the Upper Triassic and Lower Jurassic of north Victoria Land, East Antarctica, with sample and slide number and England Finder coordinates. Scale bar = 50 µm.

- 1: *Annulispora folliculosa* (Rogalska) de Jersey; GIX-TI13/5-54; G40/0.
- 2: *Annulispora microannulata* de Jersey; GIX-SHB07alt-51; E54/4.
- 3: *Rogalskaisporites cicatricosus* (Rogalska) Danzé-Corsin et Laveine; GIX-SHA08/1-52; X43/0.
- 4: *Foveosporites moretonensis* de Jersey; GIX-SHA08/5-54; C30/1.
- 5: *Stereisporites antiquasporites* (Wilson et Webster) Dettmann; GIX-TI13/5-52; R57/0.
- 6: *Stereisporites psilatus* (Ross) Pflug; GIX-SHA11-51; W49/3.
- 7: *Nevesisporites vallatus* de Jersey et Paten (*N. vallatus* var. 1106 of Price, 1997); GIX-CE34-56; V21/2.
- 8: *Antulsporites varigranulatus* (Levet-Carret) Reiser et Williams; GIX-SHA11-51; J48/1.
- 9: *Polycingulatisporites radiatus* Zhang et Grant-Mackie; GIX-AR00-55; H47/2.
- 10: *Polycingulatisporites crenulatus* Playford et Dettmann; GIX-SHA11-52; W45/4.
- 11: *Antulsporites saevus* (Balme) Archangelsky et Gamarro; GIX-SHB07-56; C24/0.
- 12: *Striatella seebergensis* Mädlér; GIX-CE34-56; V39/1.
- 13, 14: *Striatella jurassica* Mädlér; (13) GIX-SB08-58; X41/1. (14) GIX-SB08-54; V29/0.
- 15: *Densoisporites playfordii* (Balme) Dettmann; GIX-CEL13-52; H46/0.
- 16: *Limbosporites denmeadii* (de Jersey) de Jersey and Raine; GIX-TI13/5-59; H51/0.
- 17: *Marattisporites scabratus* Couper; GIX-AR00-54; U39/0.
- 18: *Punctatosporites walkomii* de Jersey; GIX-AR00-54; W54/1.
- 19: *Thymospora ipsviciensis* (de Jersey) Jain; GIX-AR00-53; L52/0.
- 20: *Tuberculatosporites aberdarensis* de Jersey; GIX-AR00-53; L30/3.
- 21: *Aratrisporites parvispinosus* Leschik; GIX-TI13/5-56; R48/3.

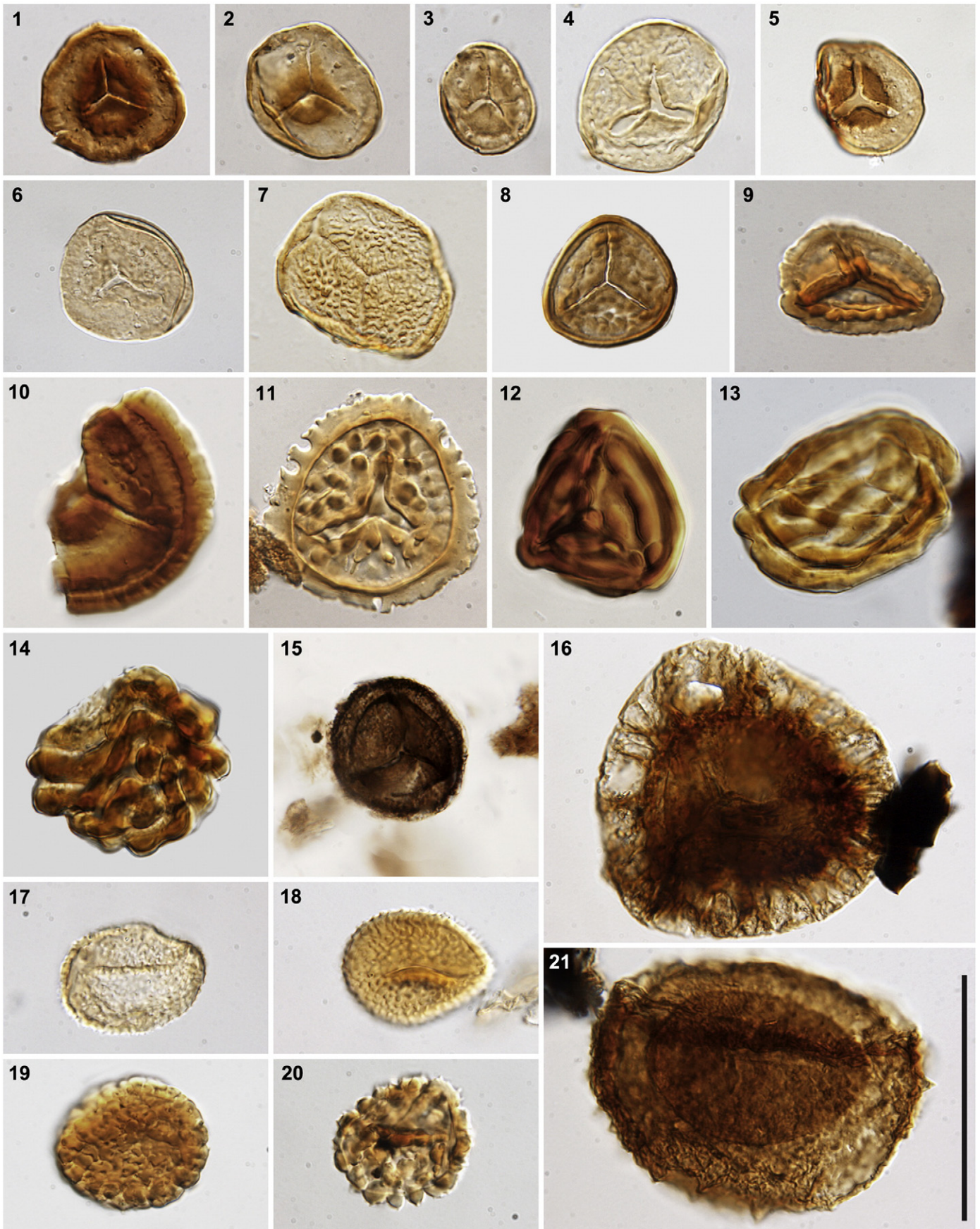


(Plate I, 3), *Osmundacidites wellmanii* (Plate I, 4) and a tentative record of *Ashmoripollis reducta*.

Discussion: The dominance of *Alisporites* spp., together with the co-occurrence of *Craterisporites rotundus*, *Polycingulatisporites crenulatus*, and *Antulsporites varigranulatus* allows assignment of samples AR00 and TI13/5 to APT5M and to subzone D of the informal Antarctic *Alisporites* zone (Kyle, 1977; Kyle and Schopf, 1982).

In south-eastern Queensland, *Polycingulatisporites crenulatus* appears in the Rhaetian at the (unconformable) base of the Bundamba Group, whereas in New Zealand the species has been reported from as low in the section as the Otamitan (early middle Norian); in both regions the species extends into the Jurassic (de Jersey and Raine, 1990; McKellar, in press). In Antarctica, this species defines the (Rhaetian) subzone D of the *Alisporites* zone (Kyle, 1977; Kyle and Schopf, 1982). Further age constraints are provided by certain taxa, that are here newly reported from East Antarctica, namely *Antulsporites varigranulatus*, *Cadargasporites reticulatus*, and *Polycingulatisporites radiatus*. In New Zealand, *A. varigranulatus* first appears in the Aratauran (Hettangian–early Sinemurian) (Zhang and Grant-Mackie, 2001). In south-eastern Queensland, it has been recorded from the Eddystone beds (named by Price et al., 1985) in drill hole GSQ Eddystone 1, in an assemblage assigned by McKellar (1978) to Assemblage A of de Jersey (1976) and correlated with otherwise similar assemblages of Rhaetian age from the basal Bundamba Group (Aberdare Conglomerate and Raceview Formation) in the Clarence–Moreton Basin. *Polycingulatisporites radiatus* has been recorded from the Otapirian (Rhaetian) and Aratauran (Hettangian–early Sinemurian) of New Zealand (Zhang and Grant-Mackie, 2001), although, according to de Jersey and McKellar (2013), the Otapirian occurrences have yet to be substantiated. It has also been reported from the Hettangian and early Sinemurian of south-eastern Queensland (de Jersey and McKellar, 2013). To our knowledge, the oldest reliable record of *C. reticulatus* is from the Rhaetian basal Bundamba Group (in the Raceview Formation palynoflora; de Jersey, 1970, 1971).

Additional assemblage references: Sample L3451 of Norris (1965) from the middle part of the Section Peak Formation at Timber Peak. The only other palynological assemblages from the Transantarctic Mountains referred to this assemblage type are those of samples 25447 and 25449 from member D of the Lashly Formation of SVL (Kyle, 1977; see Kyle and Schopf, 1982) and of the uppermost sample from the Falla Formation in the CTM described in Kyle and Fasola (1978; see Kyle and Schopf, 1982).

Radiometric age constraints: The age distribution of detrital zircons from a sandstone bed ca 10 m above the sampled horizon TI13/5 at Timber Peak contains a youngest peak of 202 ± 3 Ma (Elsner et al., 2013), which is in accordance with a latest Triassic age for this part of the Section Peak Formation.

5.2. APJ1 assemblages (Sinemurian)

Stratigraphic occurrence (Fig. 2): Upper part of the Section Peak Formation at the Priestley Glacier cliff (PR01, PR03b); Section Peak Formation at Section Peak (SPL).

Description: Samples from coal-bearing, fine-grained intercalations in the upper part of the Section Peak Formation in the Priestley Glacier area (PR01, PR03b) and from Section Peak have yielded low-diversity palynofloras (Fig. 5) that are strongly dominated by intrastriate *Classopollis* spp. (Plate III, 14, 15; reaching >90% in PR03b). *Retitriletes austroclavatidites* (Plate I, 15) occurs in sample PR03b; a further questionable record occurs in PR01. Sample SPL additionally contains *Retitriletes rosewoodensis* and *Anapiculatisporites helidonensis* (Plate I, 10).

Discussion: The assemblages are assigned to APJ1 (probably APJ11; Price, 1997) based on the clear dominance of intrastriate *Classopollis*

spp. and the apparent absence of *Ischyosporites punctatus* (respectively = *Corollina torosa* and *Ischyosporites crateris-punctatus* in Price, 1997). An early (post-basal)–middle Sinemurian age is thus advocated. *Retitriletes austroclavatidites* and *Anapiculatisporites helidonensis* (*Ceratosporites helidonensis* in Price, 1997; Plate I, 10) are also present in these assemblages, which further conform with the *Classopollis* Abundance Subzone of de Jersey and McKellar (2013). The indicated age is thus suggested for the middle part of the coal-bearing sequence in the Deep Freeze Range (ca 120 m above local basement level), as well as for the sandstone and intercalated lacustrine layers at Section Peak (ca 30 m above local basement level).

Additional assemblage references: Samples L3570 and L3571 of Norris (1965) and samples PR2, SP1, and SP3 of Pertusati et al. (2006), all from the Section Peak Formation at Section Peak.

Radiometric age constraints: Radiometric ages of detrital zircons have been obtained from two conglomeratic layers at Section Peak: the lower layer, ca 20 m above local basement and ca 10 m below our sample SPL, yielded a youngest-zircon population with peak ages of 191 ± 4 Ma (sample SP-4 in Goodge and Fanning, 2010); subsequent analysis of a sample from similar stratigraphic position yielded older maximum depositional ages of 214 ± 3 Ma (sample SP08 in Elsner et al., 2013). Another sampled horizon, ca 15 m above our sample SPL, contains a youngest-zircon population with peak ages of 198 ± 2 Ma (sample SPP36 in Elsner et al., 2013). Radiometric age data thus agree very well with our palynostratigraphic assessment assigning this part of the Section Peak Formation to the Sinemurian.

5.3. APJ2 assemblages (late Sinemurian–middle Pliensbachian)

Stratigraphic occurrence (Fig. 2): Uppermost part of the Section Peak Formation at Shafer Peak (samples SHA06, SHA08/1, SHA08/5, SHA11, SHA13).

Description: All samples from the uppermost part of the Section Peak Formation at the Shafer Peak section have yielded rich palynological assemblages (Fig. 5). These are generally characterized by a lower abundance of *Classopollis* compared to those of the underlying APJ1 assemblages, and also contain abundant *Retitriletes* spp. as well as common *Podosporites variabilis* (Plate III, 11, 12), *Podocarpidites* spp. (Plate III, 8), and *Ischyosporites punctatus* (Plate I, 17).

Discussion: Regarding the rich and generally well-preserved palynofloras from Shafer Peak, dominance of intrastriate *Classopollis* spp. (= *Corollina torosa* in Price, 1997), together with the consistent occurrences of *Podosporites variabilis* (= *Podosporites tripakshii* in Price, 1997) and *Ischyosporites punctatus* (= *Ischyosporites crateris-punctatus* in Price, 1997) enables their broad assignment to APJ2.

Radiometric age constraints: A tuffitic layer, bracketed between samples SHA11 and SHA13 at the Shafer Peak section, has yielded a U–Pb (SHRIMP) age of 188.2 ± 2.2 Ma (Elsner, 2010), equating with the early Pliensbachian.

5.4. Uppermost APJ22 assemblages (middle Pliensbachian)

Stratigraphic occurrence (Fig. 2): Lower Exposure Hill-type deposits at Shafer Peak (sample SHB07), Mount Carson E (sample CEL13), and an unnamed peak in the Deep Freeze Range that we informally refer to as ‘3350’ (sample 3310); middle to upper parts of the Shafer Peak Formation at Mount Carson E (sample CE34), Mount Carson N (CN08), and possibly Shafer Peak (SHC32).

Description: Sample SHB07, which occurs at the top of lower Exposure Hill-type deposits and is in turn directly overlain by the Shafer Peak

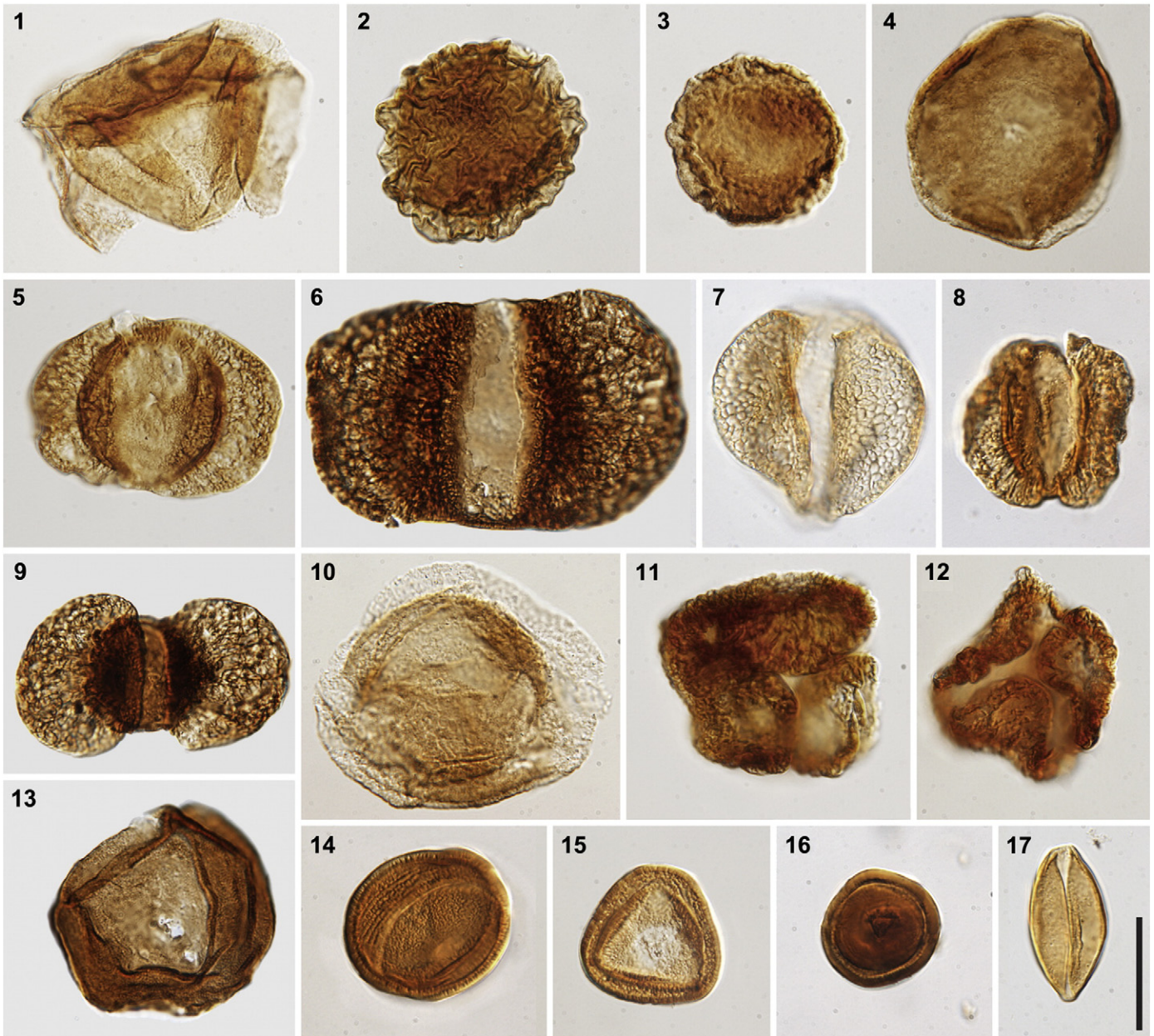


Plate III. Composite micrographs of selected pollen taxa from the Upper Triassic and Lower Jurassic of north Victoria Land, East Antarctica, with sample and slide number and England Finder coordinates. Scale bar = 25 μ m.

- 1: *Callialasporites turbatus* (Balme) Schulz; GIX-CE34-\$3; F30/3.
- 2: *Callialasporites minus* (Tralau) Guy; GIX-CE34-\$3; Q36/2.
- 3: *Callialasporites segmentatus* (Balme) Srivastava; GIX-CE34-\$6; V34/0.
- 4: *Callialasporites microvelatus* Schulz; GIX-CE34-\$3; U31/0.
- 5: *Alisporites lowoodensis* de Jersey; GIX-TI13/5-\$1; X36/0.
- 6: *Alisporites australis* de Jersey; GIX-TI13/5-\$1; T49/1.
- 7: *Indusiisporites parvisaccatus* (de Jersey) de Jersey; GIX-CE34-\$4; X49/2.
- 8: *Podocarpidites* sp.; GIX-SHA08/1-\$1; K47/4.
- 9: *Platysaccus queenslandii* de Jersey; GIX-TI13/5-\$2; M51/0.
- 10: *Perinopollenites elatoides* Couper; GIX-CE34-\$4; H40/0.
- 11, 12: *Podosporites variabilis* Sukh Dev; (11) GIX-SHA11-\$2; D43/0. (12) GIX-SHA11-\$3; 13Q52/0.
- 13: *Araucariacites australis* Cookson; GIX-TI13/5-\$1; N47/0.
- 14: *Classopollis classoides* Pflug; GIX-SHB07alt-\$1; X53/0.
- 15: *Classopollis meyerianus* (Klaus) de Jersey; GIX-SHA11-\$1; N47/1.
- 16: *Classopollis simplex* de Jersey et Paten; GIX-SHA08/1-\$2; J56/3.
- 17: *Cycadopites follicularis* Wilson et Webster; GIX-SHA08/5-\$2; X36/3.

Formation, has yielded a very well-preserved and rich palynoflora (Fig. 5); it is similar in overall assemblage composition to samples SHA08/1 and SHA08/5 from the underlying Section Peak Formation, but additionally contains *Foraminisporis tribulosus*, *Antulsporites saevus*

(Plate II, 11), and the first occurrence of *Callialasporites* (*Callialasporites segmentatus*, Plate III, 3).

Another rich and well-preserved palynological assemblage was recovered from a mudstone intercalation in the middle part of the Shafer

Peak Formation at Mount Carson E (sample CE34) (Figs. 2, 5). This assemblage is characterized by dominance of *Classopollis* (64.6%), by the common occurrence of a form of *Nevesisporites vallatus* with radiating proximal rugulae in the contact areas (*N. vallatus* var. 1106 of Price, 1997) (Plate II, 7), and by a high diversity of *Callialasporites* [including *Callialasporites turbatus* (Plate III, 1), *Callialasporites minus* (Plate III, 2), *Callialasporites segmentatus* (Plate III, 3), *Callialasporites microvelatus* (Plate III, 4), and *Callialasporites trilobatus*]. Sample CN08 from Mount Carson N is characterized by a dominance of fern spores (including mainly species of *Cyathidites*, *Dictyophyllidites*, and *Foveogleichenioidites*), by lesser amounts of *Classopollis* (22.0%), and by the consistent occurrence of *C. segmentatus*.

Sample CEL13, collected from pyroclast-bearing carbonaceous mudstone underneath the Shafer Peak Formation at the eastern ridge of Mount Carson, has yielded a poorly preserved and moderately diverse palynoflora (Fig. 5) that is dominated by *Classopollis* spp., with a high proportion of *Densoisporites* spp. (25%; Plate II, 15) and occasional *Ischyosporites punctatus* and *Podocarpidites* spp. (Plate III, 8).

Sample 3310 is from a thin pyroclast-bearing carbonaceous siltstone bed intercalated in the middle portion of a ca 200 m thick sequence of mafic volcanoclastic deposits. This sample yielded a sparse and moderately preserved palynoflora (Fig. 5) dominated by fern spores (e.g., *Dictyophyllidites* spp., *Osmundacidites wellmanii*) and lycophyte spores (*Cadargasporites granulatus*, *Densoisporites* spp.). In addition, the sample contains *Classopollis simplex* (Plate III, 16), *Classopollis meyerianus* (Plate III, 15), *Ischyosporites punctatus*, *Podocarpidites* spp., and *Retitritiles austroclavatidites*.

Residues of a bulk-macerated sample from a volcanoclastic siltstone at Shafer Peak (SHC32) yielded a low-diversity assemblage (Fig. 5) of light-coloured palynomorphs that is strongly dominated by *Classopollis* (88.3%), with only a few other taxa, including *Podocarpidites* spp., *Podosporites variabilis*, *Araucariacites* sp., and a few (<5%) fern and lycopsid spores.

Discussion: *Callialasporites* makes its first appearance in sample SHB07, represented by the species *Callialasporites segmentatus*. The consistent occurrence of this genus (and of the index species *Callialasporites dampieri*) was used by Price (1997) to mark the base of APJ3 (late Pliensbachian); it has been noted, however, that other *Callialasporites* species, including *C. segmentatus*, may occur sporadically in the upper part of APJ2 in Australia (Price, 1997) and New Zealand (de Jersey and Raine, 2002; N.J. de Jersey, personal communication, 2013). The occurrence of *Antulsporites saevus* further places this and the overlying palynofloras into the uppermost part of APJ22 (Price, 1997). The richest and biostratigraphically most informative palynoflora from the Shafer Peak Formation is the CE34 assemblage (Figs. 2, 5); the high diversity of *Callialasporites*, excluding *C. dampieri*, and the consistent occurrence of *Nevesisporites vallatus* (var. 1106 of Price, 1997) confirm a position in the uppermost part of APJ22 (Price, 1997), somewhat below the upper limit of the *Classopollis* acme in the lower Toarcian (de Jersey and McKellar, 2013).

Samples CEL13 and 3310 contain abundant *Classopollis* and *Ischyosporites punctatus*, but lack the APJ2 index species, *Podosporites variabilis*; they may be indicative of unit APJ12 (middle Sinemurian). The stratigraphic significance of these two samples, however, is questionable. Field relationships indicate that both samples derive from approximately the same stratigraphic level as the SHB07 palynoflora from Shafer Peak (Fig. 2), i.e., they represent lower Exposure Hill-type deposits. The low yield and the variable, but overall rather poor preservation of palynomorphs in both samples, and particularly the darker colour of *Densoisporites* sp. from the CEL13 sample (Plate II, 15), may indicate significant reworking. Finally, both beds contain scoria fragments and occur above very coarse-grained mafic pyroclastic deposits. We therefore consider it likely that (at least parts of) the palynomorph contents of these samples may derive from accessory clasts of underlying host strata that were incorporated and reworked during hydrovolcanic activity.

The unusual composition of the SHC32 palynoflora (Fig. 5), which is strongly dominated by *Classopollis* and lacks index taxa for upper APJ22, may have resulted from the different sample protocol applied to it: in order to obtain a sufficient number of palynomorphs from this bed, we collected the residue of a sample that had been bulk-macerated for analysis of dispersed cuticles. The light colour and the overwhelming dominance of conifer pollen (e.g., *Classopollis*, *Podocarpidites*, *Podosporites*, *Araucariacites*) might indicate that the long acid treatment during bulk maceration may have caused dissolution of more delicate palynomorphs, and thus skewed the palynomorph composition towards more robust conifer pollen types.

Additional assemblage references: Palynofloras described by Musumeci et al. (2006) from fossiliferous black shale at Shafer Peak (presumably from the same level as the SHB07 palynoflora described here).

Radiometric age constraints: No radiometric ages have been obtained from the Shafer Peak Formation to date (Elsner, 2010). However, four samples of tuff layers from the Hanson Formation, a local equivalent of the Shafer Peak Formation in the CTM, have yielded a poorly constrained middle Pliensbachian age (186 ± 8 Ma; Faure and Hill, 1973; see Elliot, 2000). Although this date is considered uncertain due to widespread zeolitization (Elliot, 2000), it completely matches the palynological age determined here. More recently, a slightly younger U–Pb SHRIMP age of 182.7 ± 1.8 Ma (late Pliensbachian/early Toarcian) has been obtained from a clast of silicic tuff (presumably Hanson Formation) from mafic volcanoclastic deposits in the Otway Massif, CTM (Elliot et al., 2007).

Successions of silicic volcanoclastic sandstone and tuff, interbedded mafic volcanoclastic deposits, and extrusive basaltic andesite with associated intrusive hyaloclastic breccias have recently been described from outcrop and drill-core sections near Lune River, Tasmania (Bromfield et al., 2007). Based on field relationships with bounding strata, age, and distinctive geochemical composition, these successions have been correlated to basal sections of Kirkpatrick Basalt in the TAM (Bromfield et al., 2007). Indeed, U–Pb ages of detrital zircons indicate a maximum deposition age of 182 ± 4 Ma for the silicic volcanoclastic deposits (Bromfield et al., 2007), congruent with the latest Pliensbachian–early Toarcian age of the silicic tuff clast from the CTM mentioned above. Moreover, plant-fossil assemblage from the Lune River site appear strikingly similar in composition and preservational aspect to those recently described from the Shafer Peak Formation of NVL (Bomfleur et al., 2011a,b; Bomfleur, pers. obs., 2006).

5.5. APJ31 assemblages (late Pliensbachian–early Toarcian)

Stratigraphic occurrence (Fig. 2): upper Exposure Hill-type deposits directly underlying the base of the Kirkpatrick Basalt at Suture Bench (sample SB08); sedimentary interbed between Kirkpatrick Basalt flows at Mount Fazio (sample 82-5-14).

Description: Sample SB08 is from a bed of olive-green claystone directly underlying the lowermost pillow lavas at Suture Bench. This horizon occurs above coarse-grained mafic volcanoclastic deposits that in turn overlie an, at least, 8 m thick succession of reworked silicic ashes of the Shafer Peak Formation (Fig. 2). The SB08 palynoflora is rather poorly preserved and light-yellow in colour. The assemblage is marked by a decrease in *Classopollis* (22.5%) compared to the underlying APJ2 assemblages, by a high abundance of *Klukisporites variegatus* (19.1%; Plate I, 16) and *Ischyosporites punctatus* (12.4%), and by common cf. ‘*Concavissimisporites–Impardecispora*’ sp. (Plate I, 6–8) and cf. *Trilobosporites antiquus* (Plate I, 18). In addition, this assemblage contains *Striatella seebergensis* (Plate II, 12) and *Striatella jurassica* (Plate II, 13, 14), as well as *Callialasporites turbatus* (Plate III, 1), *Callialasporites minus* (Plate III, 2), and *Callialasporites trilobatus*.

Of six processed samples from the Kirkpatrick Basalt interbeds, only sample 82-5-14 from Mount Fazio yielded palynomorphs; these include a few *Classopollis* grains, *Osmundacidites* spores, *Callialasporites minus*, and the biostratigraphically significant *Densosporites* sp. A (of Filatoff, 1975) and *Phlebopterisporites equiexinus*.

Discussion: We place the SB08 palynoflora into lower APJ3 of Price (1997; late Pliensbachian to early Toarcian), based on still abundant *Classopollis*, on the diversity of *Callialasporites*, and on the particular composition of cryptogam spores, which includes *Klukisporites variegatus*, *Ischyosporites punctatus*, cf. *Trilobosporites antiquus*, and *Striatella jurassica* (Fig. 5). Similar spore assemblages have been described to be a distinct, facies-controlled association (upper Poolowanna assemblages) in the lower part of unit APJ3 in the Eromanga Basin of eastern Australia (Price, 1997). The specimens that we here provisionally list as cf. ‘*Concavissimisporites–Impardecispora*’ sp. probably represent a new species. They are similar to some late Early Jurassic or younger taxa (see, e.g., *Concavissimisporites verrucosus*, *Impardecispora apiverrucata*, or *Converrucosporites* spp. nov. of McKellar, in press; Geoff Wood, personal communication, 2013); the insufficient preservation, however, hampers generic assignment and clear taxonomic delimitation.

The low yield and poor preservation of palynomorphs from sample 82-05-14 make an age assignment difficult. *Densosporites* sp. A of Filatoff (1975), however, is reported by McKellar (in press) from the north-western Surat Basin as a new species that first appears in his Toarcian *Araucariacites fissus* Association Zone.

Palynofloras reported from other Kirkpatrick Basalt interbeds at Carapace Nunatak (Tasch and Lammons, 1978; Shang, 1997; Ribecai, 2007), Storm Peak (Tasch and Lammons, 1978), and Coalsack Bluff (Tasch and Lammons, 1978) are remarkably similar to the SB08 palynoflora here described from upper Exposure Hill-type deposits at Suture Bench. All share the relatively high amount of *Classopollis*, presence of various *Callialasporites* species, and the particular “upper Poolowanna”-type spore composition (Tasch and Lammons, 1978; Shang, 1997; Ribecai, 2007). Some of the Kirkpatrick Basalt interbeds

were suggested to be late Middle Jurassic in age (Shang, 1997; Ribecai, 2007), based on the alleged presence of *Contignisporites cooksonii*. Price (1997), however, emphasized that *Contignisporites* is easily confused with some late Early Jurassic species of *Striatella*, including *Striatella jurassica* recorded and figured herein. We therefore suggest that earlier reports of *Contignisporites* from the Kirkpatrick Basalt interbeds, interpreted as indicating a late Middle Jurassic age (Shang, 1997; Ribecai, 2007) incompatible with the radiometric data (see Pálffy and Smith, 2000; Riley and Knight, 2001), may in fact refer to Early Jurassic occurrences of *Striatella* spp.

Additional assemblage references: Samples that we consider as coming from probably equivalent strata in other regions of the TAM include CP6a-g and CP7a-f of Ribecai (2007) from the Carapace Sandstone at Carapace Nunatak, SVL; assemblage A–B–C of Tasch and Lammons (1978), samples F1, F2, and F3 of Shang (1997), and sample CRN of Ribecai (2007) from the basal interbeds in the Kirkpatrick Basalt at Carapace Nunatak, SVL; and assemblages D–E–F and G of Tasch and Lammons (1978) from sedimentary interbeds in the Kirkpatrick Basalt at Storm Peak and Coalsack Bluff.

Radiometric age constraints: Radiometric ages of Kirkpatrick Basalt rocks have been obtained from various localities in the Transantarctic Mountains (see Riley and Knight, 2001). Two samples from the uppermost (youngest) flow at Mount Frustrum and at Gair Mesa (Foland et al., 1993; Heimann et al., 1994), in close vicinity to our palynological sample sites at Suture Bench and Mount Fazio, have yielded ages respectively of 180.0 ± 1.3 Ma and 180.4 ± 1.2 Ma (recalculated in Riley and Knight, 2001, with the revised standards of Renne et al., 1994). Other samples of Kirkpatrick Basalt flows from SVL and the CTM (Heimann et al., 1994; Elliot et al., 1999) have provided similar ages ranging from 178.5 ± 0.7 Ma to 180.0 ± 0.7 Ma (Riley and Knight, 2001). In addition, a sample from pillow basalt at the base of the lava pile at Carapace Nunatak, SVL (Foland et al., 1993), at a stratigraphic position equivalent to the pillows overlying sample SB08 from Suture Bench, yielded a closely comparable radiometric age of 180.2 ± 0.7 Ma (Riley

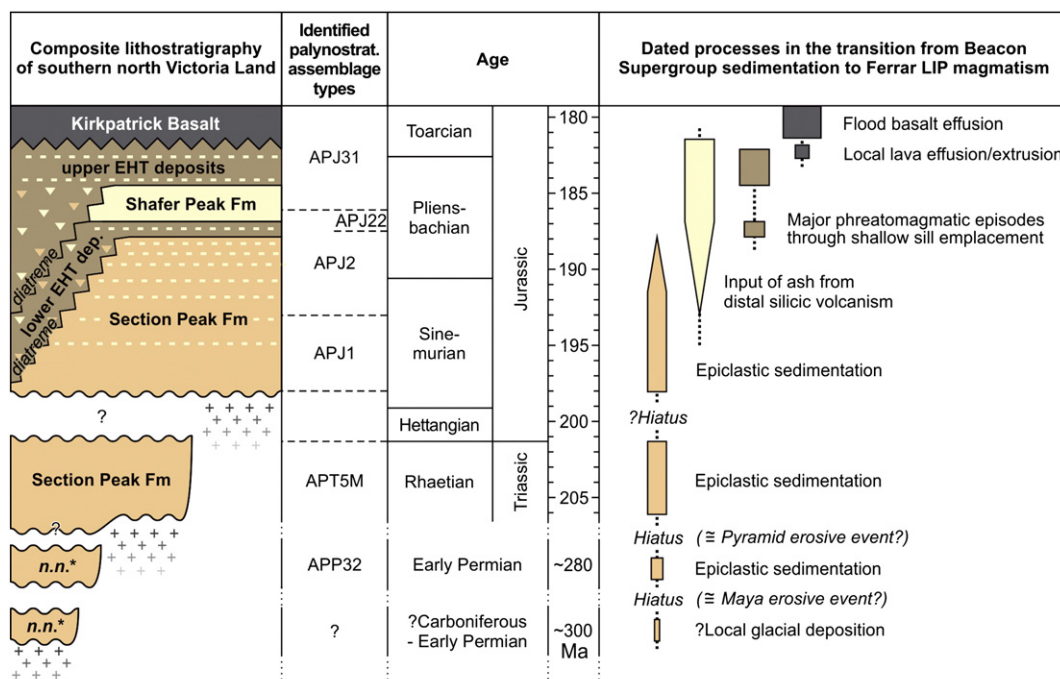


Fig. 6. Timeline of major sedimentary and magmatic events in north Victoria Land as inferred from the identified palynostratigraphic assemblage types in an idealized, composite stratigraphic column. *Putative Palaeozoic units (labelled “n. n.”) in the Eisenhower Range area have only recently been identified (Bomfleur et al., 2014), and are still unnamed. Note that diagonal zigzag lines in the basal contacts of EHT deposits on the left indicate erosional unconformities bounding diatreme structures.

and Knight, 2001). Hence, all available radiometric data collectively point to a very short-lived extrusive/effusive phase of the Kirkpatrick Basalt during the early Toarcian at ca 180 Ma (Heimann et al., 1994; Pálffy and Smith, 2000; Riley and Knight, 2001). Our assessment that all palynofloras occurring in between or directly underneath the pile of Kirkpatrick Basalt can be assigned to the late Pliensbachian–early Toarcian APJ31 zonal unit thus agrees well with this radiometric evidence.

6. Discussion

6.1. Deposition of the Section Peak Formation

Altogether, the age of the Section Peak Formation in southern NVL can be constrained to the Rhaetian to middle Pliensbachian interval (Fig. 6). However, within this interval, to date, there is no evidence in NVL of Hettangian (–earliest Sinemurian) palynofloras [attributable to APT5U and the equivalent *Toripustulatisporites hokonuiensis* Association Zone (discussed above)] that have been described from easternmost Australia (de Jersey and McKellar, 2013). According to the latter authors, a hiatus appears to consume the Hettangian (–lowermost Sinemurian) across most of the Australian continent, as is generally the case on a global scale, there thus being widespread unconformity at the Triassic–Jurassic boundary. This therefore has major implications for the System boundary in NVL, with the inference that Hettangian (–earliest Sinemurian) strata may also be missing there too.

6.2. Implications for the onset of magmatism in the Ferrar Large Igneous Province

The earliest evidence for igneous activity in the Ferrar Province is documented in NVL by intercalations of reworked rhyolitic tuff in the uppermost Section Peak Formation (Schöner et al., 2007, 2011). Presumably, the lowest tuffitic layers occur at the Priestley Glacier cliff; intercalated mudstones yielded early (post-earliest)–middle Sinemurian palynofloras (PR01 and PR03b). At Shafer Peak, a tuffitic siltstone layer in the upper Section Peak Formation is conformably overlain by a mudstone containing a late Sinemurian–middle Pliensbachian palynoflora (SHA06). The onset of the following large-volume input of distal silicic ashes, represented by the overlying Shafer Peak Formation, can be constrained to the middle Pliensbachian (uppermost APJ22). Hence, our data indicate that explosive silicic volcanism began with minor pulses as early as ca 195 Ma, and culminated during an interval of peak silicic volcanism beginning at ca 187 Ma (Fig. 6). The common occurrences of admixed silicic volcanic material in the otherwise mafic volcanoclastic deposits and in basalt interbeds throughout the TAM (Elliot et al., 1986a,b; Wörner, 1992; Elliot, 2000; Bromfield et al., 2007; Elliot et al., 2007; Viereck-Goette et al., 2007; Elliot and Fleming, 2008), together with radiometric ages of silicic clasts from the CTM and Tasmania, document that silicic volcanism lasted until at least ca 182 Ma. This demonstrates a close temporal link to the first magmatic episode of the Chon Aike province (Bryan et al., 2002), which occurred between ca 189–178 Ma in the southern Antarctic Peninsula region (Pankhurst et al., 2000; Riley et al., 2001; Hunter et al., 2006), and between ca 187 and 182 Ma in north-eastern Chubut and Rio Negro Province, Patagonia (Féraud et al., 1999; Pankhurst et al., 2000).

Mafic volcanoclastic deposits in the TAM can be regarded as the sub-aerial expression of shallow-level sill intrusions, because the deposits formed through explosive water–magma interaction when ascending sills or sill apophyses reached into wet Beacon Supergroup sediments (Viereck-Goette et al., 2007; Elliot and Fleming, 2008; see Muirhead et al., 2012). Viereck-Goette et al. (2007) recognise two major pulses of sill intrusion prior to lava effusion in NVL. Our data indicate that the first pulse, documented by the lower Exposure Hill-type deposits at the base of the Shafer Peak Formation, took place during the middle Pliensbachian at around 187 Ma; the second major pulse of shallow-

level sill emplacement can be constrained to a time interval between ca 185 and 180 Ma (late Pliensbachian–early Toarcian), which is congruent with radiometric ages dating the intrusion of the Ferrar Dolerite to ca 183 Ma (Encarnación et al., 1996; Muirhead et al., 2012) (Fig. 6). This second episode was also accompanied by small-scale Strombolian eruptions (Viereck-Goette et al., 2007), which may indicate a rise in magma supply and intrusion level. The subsequent emplacement of the Kirkpatrick Basalt began with local lava effusion and pillow extrusion in small volcanic centres (Viereck-Goette et al., 2007). Sedimentary interbeds between initial lava flows have yielded well-preserved palynofloras from Carapace Nunatak, Storm Peak, and Coalsack Bluff (Tasch and Lammons, 1978; Shang, 1997; Ribecai, 2007). Some of these palynofloras were interpreted as indicating a late Middle Jurassic age (Shang, 1997; Ribecai, 2007), probably because the common *Striatella* species have been confused with the typically late Middle Jurassic index form *Contignisporites* (see Price, 1997; McKellar, in press). In fact, the palynofloras from these sedimentary interbeds are essentially similar to those from Exposure Hill-type deposits below the Kirkpatrick Basalt. In conclusion, all present palynological evidence agrees very well with the radiometric data, indicating a short-lived emplacement of the Kirkpatrick Basalt during the earliest Toarcian at ca 180 Ma (Pálffy and Smith, 2000; Riley and Knight, 2001) (Fig. 6).

7. Summary and conclusions

The occurrence of surprisingly well-preserved palynofloras in the sedimentary successions of the TAM contradicts previous assumptions that thermal alteration during LIP magmatism would have made these host rocks unsuitable for palynological analyses (e.g., Kyle, 1977; Kyle and Fasola, 1978; Kyle and Schopf, 1982). The palynological assemblages allow us to characterize the timing of individual processes that ultimately lead from epiclastic sedimentation in the Transantarctic Basin to flood-basalt effusion in the Ferrar Large Igneous Province in far greater detail than previously known. Our data indicate that during the Mesozoic, onset of deposition of the Beacon Supergroup was asynchronous across southern north Victoria Land, ranging from at least the latest Triassic in central parts of the basin to Early Jurassic at the cratonward basin margin (Figs. 2, 6). With a putative hiatus during the Hettangian (–earliest Sinemurian), primarily epiclastic sedimentation then lasted until the late Sinemurian, with first intercalations of distal silicic ashes occurring already in the (post-basal) lower Sinemurian. The Beacon Supergroup succession is overlain by a package of reworked distal silicic ashes that we date as middle Pliensbachian to possibly early Toarcian (Fig. 6), indicating a strikingly close temporal link to the early magmatic phase of the Chon Aike province in West Antarctica and Patagonia. Sill intrusions into wet sediments triggered explosive hydrovolcanism that produced the mafic volcanoclastic deposits widespread throughout the Transantarctic Mountains. We dated lacustrine deposits overlying mafic pyroclastic breccias at several localities, and recognise two major phases of phreatomagmatic activity: one occurring during the middle Pliensbachian and the other during the late Pliensbachian to early Toarcian (Fig. 6). These phreatomagmatic episodes represent the first sub-aerial expression of mafic magmatic activity in the Ferrar Large Igneous Province. The emplacement of the Kirkpatrick Basalt during the early Toarcian began with local lava effusion and pillow extrusion, followed by the massive outpouring of the plateau-forming flood basalts (Fig. 6).

Acknowledgements

We thank the Bundesanstalt für Geowissenschaften und Rohstoffe (BGR, Hannover), for the invitation to join the GANOVEX IX expedition, and for generous logistical support and a great time in the field. Technical support during field work by the Alfred-Wegener-Institut für Meeres- und Polarforschung (AWI), Bremerhaven, is gratefully acknowledged. We wish to thank D.H. Elliot (Columbus, OH) for providing

palynological samples from Kirkpatrick Basalt interbeds collected during the 1981/1982 US–New Zealand–Australia Joint International Expedition; Noel J. de Jersey (retired, previously of the Geological Survey of Queensland) for very helpful discussion on the subdivision and dating of the south-eastern Queensland and New Zealand Late Triassic–Early Jurassic palynostratigraphic successions; Geoff Wood of Santos Ltd (Adelaide) for help with the identification of cf. *Concavissimiporites–Impardecispora* sp.; Nigel Ellis and Christine Klimek (Lune River, Tasmania) for an enjoyable field excursion to the Lune River site and for access to their superb collection of plant fossils from the area; Cindy Looy (Berkeley, CA) for assistance in obtaining literature; and an anonymous reviewer for a detailed and critical evaluation of an earlier version of this manuscript. Financial support has been provided by the Deutsche Forschungsgemeinschaft [DFG grants KE584/12-1, 16-1, and 16-2; GA457/11-1, 13-2, and 13-3; SCHN408/11-1, 13-2, and 13-3; VI215/6-1, 6-2, and 6-3; all in Priority Programme 1158: Antarctic Research with comparative investigations in Arctic ice areas (<http://www.spp-antarktisforschung.de/>)].

Appendix A. Alphabetical list of taxa identified during this study

- Alisporites australis* (de Jersey) Stevens 1981 (Plate III, 6)
Alisporites lowoodensis de Jersey 1963 (Plate III, 5)
Anapiculatisporites cooksonae Playford 1965
Anapiculatisporites helidonensis (de Jersey) de Jersey et McKellar 2013 (Plate I, 10)
Anapiculatisporites pristidentatus Reiser et Williams 1969
Annulispora folliculosa (Rogalska) de Jersey 1959 (Plate II, 1)
Annulispora microannulata de Jersey 1962 (Plate II, 2)
Antulsporites saevus (Balme) Archangelsky et Gamero 1966 (Plate II, 11)
Antulsporites varigranulatus (Levet-Carette) Reiser et Williams 1969 (Plate II, 8)
Apiculatisporis globosus (Leschik) Playford et Dettmann 1965
Apiculatisporis levis (Balme et Hennelly) Segroves 1970
Aratrisporites banksii Playford 1965
Aratrisporites flexibilis Playford et Dettmann 1965
Aratrisporites parvispinosus Leschik 1955 (Plate II, 21)
Araucariacites australis Cookson 1947 (Plate III, 13)
Araucariacites cf. *fissus* Reiser et Williams 1969
 cf. *Ashmoripollis reducta* Helby 1966
Baculatisporites comaumensis (Cookson) Potonié 1956 (Plate I, 5)
Cadargasporites baculatus de Jersey et Paten emend. Reiser et Williams 1969 (Plate I, 12)
Cadargasporites cuyanensis Azcuy et Longobucco 1983
Cadargasporites granulatus de Jersey et Paten emend. Reiser et Williams 1969
Cadargasporites reticulatus de Jersey et Paten 1964 (Plate I, 13)
Cadargasporites senectus de Jersey et Hamilton 1967 (Plate I, 14)
Calamospora tener (Leschik) de Jersey 1962
Callialasporites microvelatus Schulz 1966 (Plate III, 4)
Callialasporites minus (Tralau) Guy 1971 (Plate III, 2)
Callialasporites segmentatus (Balme) Srivastava 1963 (Plate III, 3)
Callialasporites trilobatus (Balme) Sukh Dev 1961
Callialasporites turbatus (Balme) Schulz 1967 (Plate III, 1)
Cibotiumspora intrastratus (Nilsson) Zhang et Grant-Mackie 1997
Cibotiumspora juriensis (Balme) Filatoff 1975
Circulisporites parvus de Jersey 1962
Classopollis classoides Pflug 1953 (Plate III, 14)
Classopollis meyerianus (Klaus) de Jersey 1973 (Plate III, 15)
Classopollis simplex de Jersey et Paten 1963 (Plate III, 16)
Concavissimiporites sp.
 cf. *Concavissimiporites–Impardecispora* sp. indet. (Plate I, 6–8)
Converrucosporites cameronii (de Jersey) Playford et Dettmann 1965
Craterisporites rotundus de Jersey 1970 (Plate I, 11)
Cyathidites australis Couper 1953 (Plate I, 2)
Cyathidites brevibradiatus Helby 1966
Cyathidites minor Couper 1953 (Plate I, 1)
Cycadopites follicularis Wilson et Webster 1946 (Plate III, 17)
 cf. *Dacrycarpites* sp.
Deltoidospora magna (de Jersey) Norris 1965
Densoisporites sp. A Filatoff 1975
Densoisporites playfordii (Balme) Dettmann 1963 (Plate II, 15)
Densoisporites psilatus (de Jersey) Raine et de Jersey 1988
Densoisporites sp.
Dictyophyllidites harrisii Couper 1958
Dictyophyllidites mortonii (de Jersey) Playford et Dettmann 1965 (Plate I, 3)
 cf. *Dijkstraiporites* sp.
 cf. *Exesipollenites tumulus* Balme 1957
Foraminisporis tribulosus Playford et Dettmann 1965
Foveogleicheniidites sp.
Foveosporites moretonensis de Jersey 1964 (Plate II, 4)
Glucheniidites senonicus Ross emend. Skarby 1964
Granulatisporites minor de Jersey 1960
Granulatisporites sp. Filatoff 1975
Inaperturopollenites spp.
Indusiisporites parvisaccatus (de Jersey) de Jersey 1963 (Plate III, 7)
Ischyosporites punctatus Cookson et Dettmann 1958 (Plate I, 17)
Klukisporites variegatus Couper 1958 (Plate I, 16)
Laevigatosporites sp.
Limbosporites antiquus (de Jersey) de Jersey et Raine 1990
Limbosporites denmeadii (de Jersey) de Jersey et Raine 1990 (Plate II, 16)
 cf. *Lundbladisporea* sp.
Marattisporites scabratus Couper 1958 (Plate II, 17)
 cf. *Matonisporites* sp.
Megamonopores sp.
Neoraistrickia ramosa (Balme et Hennelly) Hart 1960
Neoraistrickia sp. cf. *N. trichosa* Filatoff 1975
Neoraistrickia truncata (Cookson) Potonié 1956
Nevesisporites vallatus de Jersey et Paten 1964 (Plate II, 7)
Obtusisporis sp. cf. *O. canadensis* Pocock 1970
Osmundacidites wellmanii Couper 1953 (Plate I, 4)
Perinopollenites elatoides Couper 1958 (Plate III, 10)
Phlebopterisporites equiexinus (Couper) Juhász 1979
Pilisporites marcidus Balme 1957
Pityosporites antarcticus Seward 1914
Platysaccus queenslandii de Jersey 1962 (Plate III, 9)
Podocarpidites spp. (Plate III, 8)
Podosporites variabilis Sukh Dev 1961 (Plate III, 11, 12)
Polycingulatisporites crenulatus Playford et Dettmann 1965 (Plate II, 10)
Polycingulatisporites mooniensis de Jersey et Paten 1964
Polycingulatisporites radiatus Zhang et Grant-Mackie 1997 (Plate II, 9)
Protohaploxylinus samoilovichii (Jansonius) Hart 1964
 ?*Protopinus stabilis* Norris 1965
Punctatosporites walkomii de Jersey 1962 (Plate II, 18)
Retitriteles austroclavatidites (Cookson) Döring, Krutzsch, Mai et Schulz 1963 (Plate I, 15)
Retitriteles rosewoodensis (de Jersey) McKellar 1974
Retitriteles cf. *semimuris* (Danzé-Corsin et Laveine) McKellar 1974
Rogalskaisporites canaliculus Filatoff 1975
Rogalskaisporites cicatricosus (Rogalska) Danzé-Corsin et Laveine 1963 (Plate II, 3)
Rugaletes sp.
Schizosporis scissus Balme et Hennelly 1965
 cf. *Steevesipollenites claviger* de Jersey et Raine 1990
Stereisporites antiquasporites (Wilson et Webster) Dettmann 1963 (Plate II, 5)
Stereisporites psilatus (Ross) Pflug 1953 (Plate II, 6)
Striatella jurassica Mädlar 1964 (Plate II, 13, 14)
Striatella seebergensis Mädlar 1964 (Plate II, 12)
Sulcatiporites institatus Balme 1970

Sulcosaccispora lata de Jersey et Hamilton 1967

Thymospora ipsviciensis (de Jersey) Jain 1968 (Plate II, 19)

Todisporites minor Couper 1958

Trilobosporites antiquus Reiser et Williams 1969 (Plate I, 18)

Triplexisporites playfordii (de Jersey et Hamilton) Foster 1979

Tuberculosporites aberdarensis de Jersey 1962 (Plate II, 20)

Uvaesporites argenteaeformis (Bolkhovitina) Schulz 1967

Uvaesporites glomeratus Döring 1965

Uvaesporites verrucosus (de Jersey) Helby 1971 (Plate I, 9)

Verrucosisorites varians Volkheimer 1972

Vitreisporites pallidus (Reissinger) Nilsson 1958

References

- Askin, R.A., Cully, T.J., 1998. Permian to Jurassic palynological collections in the Shackleton Glacier area. *Antarct. J. US* 31, 3–5.
- Balme, B.E., 2000. Flora. In: Grant-Mackie, J.A., Aita, Y., Balme, B.E., Campbell, H.J., Challinor, A.B., MacFarlan, D.A.B., Molnar, R.E., Stevens, G.R., Thulborn, R.A., Jurassic Palaeobiogeography of Australasia. Association of Australasian Palaeontologists Memoir 23, 311–353.
- Barrett, P.J., 1991. The Devonian to Jurassic Beacon Supergroup of the Transantarctic Mountains and correlatives in other parts of Antarctica. In: Tingey, R.J. (Ed.), *The Geology of Antarctica*. Clarendon Press, Oxford, pp. 120–152.
- Bercovici, A., Hadley, A., Villanueva-Amadoz, U., 2009. Improving depth of field resolution for palynological photomicrography. *Palaeontol. Electron.* 12 (2) (12 pp. http://palaeo-electronica.org/2009_2/170/index.html).
- Bomfleur, B., Kerp, H., 2010a. *Dicroidium* diversity in the Upper Triassic of north Victoria Land, East Antarctica. *Rev. Palaeobot. Palynol.* 160, 67–101.
- Bomfleur, B., Kerp, H., 2010b. The first record of the dipterid fern leaf *Clathropteris* Brongniart from Antarctica and its relation to *Polyphacelus stormensis* Yao, Taylor et Taylor nov. emend. *Rev. Palaeobot. Palynol.* 160, 143–153.
- Bomfleur, B., Schneider, J.W., Schöner, R., Viereck-Götte, L., Kerp, H., 2011a. Fossil sites in the continental Victoria and Ferrar groups (Triassic–Jurassic) of North Victoria Land, Antarctica. *Polarforschung* 80, 88–99.
- Bomfleur, B., Pott, C., Kerp, H., 2011b. Plant assemblages from the Shafer Peak Formation (Lower Jurassic), north Victoria Land, Transantarctic Mountains. *Antarct. Sci.* 23, 188–208.
- Bomfleur, B., Schöner, R., John, N., Schneider, J.W., Elsner, M., Viereck-Götte, L., Kerp, H., 2014. New Palaeozoic deposits of the Victoria Group in the Eisenhower Range, northern Victoria Land. *Antarctica. Antarct. Sci.* 26, 277–278.
- Bradshaw, M.A., 1987. Additional field interpretation of the Jurassic sequence at Carapace Nunatak and Coombs Hills, south Victoria Land, Antarctica. *N. Z. J. Geol. Geophys.* 30, 37–49.
- Bromfield, K., Burrett, C.F., Leslie, R.A., Meffre, S., 2007. Jurassic volcanoclastic–basaltic andesite–dolerite sequence in Tasmania: new age constraints for fossil plants from Lune River. *Aust. J. Earth Sci.* 54, 965–974.
- Bryan, S.E., Riley, T.R., Jerram, D.A., Stephens, C.J., Leat, P.T., 2002. Silicic volcanism: an undervalued component of large igneous provinces and volcanic rifted margins. In: Menzies, M.A., Klemperer, S.L., Ebinger, C.J., Baker, J. (Eds.), *Volcanic Rifted Margins*. Geological Society of America Special Paper, 362, pp. 99–120.
- Casnedi, R., Di Giulio, A., 1999. Sedimentology of the Section Peak Formation (Jurassic), Northern Victoria Land, Antarctica. *Int. Assoc. Sedimentol. Spec. Publ.* 28, 435–448.
- Collinson, J.W., 1990. Depositional setting of Late Carboniferous to Triassic biota in the Transantarctic Basin. In: Taylor, T.N., Taylor, E.L. (Eds.), *Antarctic Palaeobiology: Its Role in the Reconstruction of Gondwana*. Springer, New York, pp. 1–14.
- Collinson, J.W., Pennington, C.D., Kemp, N.R., 1986. Stratigraphy and petrology of Permian and Triassic fluvial deposits in northern Victoria Land, Antarctica. In: Stump, E. (Ed.), *Geological Investigations in Northern Victoria Land*. Antarctic Research Series, 46, pp. 211–242.
- Collinson, J.W., Isbell, J.L., Elliot, D.H., Miller, M.F., Miller, J.M.G., Veevers, J.J., 1994. Permian–Triassic Transantarctic basin. In: Veevers, J.J., Powell, C.M., (Eds.), *Permian–Triassic Pangean Basins and Foldbelts Along the Panthalassan Margin of Gondwanaland*. Geological Society of America Memoir 184, 173–222.
- Cook, A.G., Bryan, S.E., Draper, J., 2013. Post-orogenic Mesozoic basins and magmatism. In: Jell, P. (Ed.), *Geology of Queensland*. Geological Survey of Queensland. Brisbane, QLD, pp. 515–576.
- Cooper, R.A., 2004. The New Zealand geological timescale. *Mon. Weather Rev.* 22.
- de Jersey, N.J., 1970. Triassic miospores from the Blackstone Formation, Aberdare Conglomerate and Raceview Formation. Geological Survey of Queensland, Publication 348. Palaeontological Paper, 25 (41 pp.).
- de Jersey, N.J., 1971. Early Jurassic miospores from the Helidon Sandstone. Geological Survey of Queensland, Publication 351. Palaeontological Paper, 25 (49 pp.).
- de Jersey, N.J., 1974. Palynology and age of the Callide Coal Measures. *Queensland Gov. Min. J.* 75, 249–252.
- de Jersey, N.J., 1975. Miospore zones in the Lower Mesozoic of southeastern Queensland. In: Campbell, K.S.W. (Ed.), *Gondwana Geology. Papers Presented at the Third Gondwana Symposium*, Canberra, Australia, 1973, pp. 159–172.
- de Jersey, N.J., 1976. Palynology and time relationships in the lower Bundamba Group (Moreton Basin). *Queensland Gov. Min. J.* 77, 460–465.
- de Jersey, N.J., McKellar, J.L., 2013. The palynology of the Triassic–Jurassic transition in southeastern Queensland, Australia, and correlation with New Zealand. *Palynology* 37, 77–114.
- de Jersey, N.J., Raine, J.L., 1990. Triassic and earliest Jurassic miospores from the Murihiku Supergroup, New Zealand. *N. Z. Geol. Surv. Paleontol. Bull.* 62 (164 pp.).
- de Jersey, N.J., Raine, J.L., 2002. Early to Middle Jurassic miospore zonation, New Zealand. *Geol. Soc. Aust.* 68, 41–42 (abstract).
- Elliot, D.H., 1996. The Hanson Formation: a new stratigraphical unit in the Transantarctic Mountains, Antarctica. *Antarct. Sci.* 8, 389–394.
- Elliot, D.H., 2000. Stratigraphy of Jurassic pyroclastic rocks in the Transantarctic Mountains. *J. Afr. Earth Sci.* 31, 77–89.
- Elliot, D.H., 2013. The geological and tectonic evolution of the Transantarctic Mountains: a review. *Geol. Soc. Lond. Spec. Publ.* 381, 7–35.
- Elliot, D.H., Fleming, T.H., 2008. Physical volcanology and geological relationships of the Jurassic Ferrar Large Igneous Province, Antarctica. *J. Volcanol. Geotherm. Res.* 172, 20–37.
- Elliot, D.H., Grimes, C.G., 2011. Triassic and Jurassic strata at Coombs Hills, south Victoria Land: stratigraphy, petrology and cross-cutting breccia pipes. *Antarct. Sci.* 23, 268–280.
- Elliot, D.H., Haban, M.A., Siders, M.A., 1986a. The Exposure Hill Formation, Mesa Range. In: Stump, E. (Ed.), *Geological Investigations in Northern Victoria Land*. Antarctic Research Series, 46, pp. 267–278.
- Elliot, D.H., Siders, M.A., Haban, M.A., 1986b. Jurassic tholeiites in the region of the Upper Rennick Glacier, North Victoria Land. In: Stump, E. (Ed.), *Geological Investigations in Northern Victoria Land*. Antarctic Research Series, 46, pp. 249–265.
- Elliot, D.H., Fleming, T.H., Kyle, P.R., Foland, K.A., 1999. Long-distance transport of magmas in the Jurassic Ferrar Large Igneous Province, Antarctica. *Earth Planet. Sci. Lett.* 167, 89–104.
- Elliot, D.H., Fleming, T.H., Foland, K.A., Fanning, C.M., 2007. Jurassic silicic volcanism in the Transantarctic Mountains: was it related to plate margin processes or to Ferrar magmatism. In: Cooper, A.K., Raymond, C.R., et al. (Eds.), *Antarctica: A Keystone in a Changing World – Online Proceedings of the 10th ISAES*. USGS Open-File Report 2007-1047, Short Research Paper, 051. <http://dx.doi.org/10.3133/of2007-1047.srp051> (5 pp.).
- Elsner, M., 2010. Triassic to Early Jurassic Sandstones in North Victoria Land, Antarctica: Composition, Provenance, and Diagenesis. PhD Thesis Friedrich-Schiller-Universität, Jena (184 pp.).
- Elsner, M., Schöner, R., Gerdes, A., Gaupp, R., 2013. Reconstruction of the early Mesozoic plate margin of Gondwana by U–Pb ages of detrital zircons from northern Victoria Land, Antarctica. *Geol. Soc. Lond. Spec. Publ.* 383, 212–232.
- Encarnación, J., Fleming, T.H., Elliot, D.H., Eales, H.V., 1996. Synchronous emplacement of Ferrar and Karoo dolerites and the early breakup of Gondwana. *Geology* 24, 535–538.
- Farabee, M.J., Taylor, E.L., Taylor, T.N., 1989. Pollen and spore assemblages from the Falla Formation (Upper Triassic), central Transantarctic Mountains, Antarctica. *Rev. Palaeobot. Palynol.* 61, 101–138.
- Farabee, M.J., Taylor, E.L., Taylor, T.N., 1990. Correlation of Permian and Triassic palynomorph assemblages from the central Transantarctic Mountains, Antarctica. *Rev. Palaeobot. Palynol.* 65, 257–265.
- Faure, G., Hill, R.L., 1973. Age of the Falla Formation (Triassic), Queen Alexandra Range. *Antarct. J. US* 8, 264–266.
- Féraud, G., Alric, V., Fornari, M., Haller, M., 1999. $^{40}\text{Ar}/^{39}\text{Ar}$ dating of the Jurassic volcanic province of Patagonia: migrating magmatism related to Gondwana break-up and subduction. *Earth Planet. Sci. Lett.* 172, 83–96.
- Filatoff, J., 1975. Jurassic palynology of the Perth Basin. *Palaeontogr. Abt. B* 154, 1–113.
- Foland, K.A., Fleming, T.H., Heimann, A., Elliot, D.H., 1993. Potassium–argon dating of fine-grained basalts with massive Ar loss: application of the $^{40}\text{Ar}/^{39}\text{Ar}$ technique to plagioclase and glass from the Kirkpatrick Basalt, Antarctica. *Chem. Geol.* 107, 173–190.
- Gair, H.S., Norris, G., Ricker, J., 1965. Early Mesozoic microfloras from Antarctica. *N. Z. J. Geol. Geophys.* 8, 231–235.
- Goodge, J.W., Fanning, C.M., 2010. Composition and age of the East Antarctic Shield in eastern Wilkes Land determined by proxy from Oligocene–Pleistocene glaciomarine sediment and Beacon Supergroup sandstones, Antarctica. *Geol. Soc. Am. Bull.* 122, 1135–1159.
- Gradstein, F.M., Ogg, J.G., Schmitz, M., Ogg, G., 2012. *The Geological Time Scale*. Elsevier, Amsterdam.
- Hanson, R.E., Elliot, D.H., 1996. Rift-related Jurassic basaltic phreatomagmatic volcanism in the central Transantarctic Mountains: precursory stage to flood-basalt effusion. *Bull. Volcanol.* 58, 327–347.
- Heimann, A., Fleming, T.H., Elliot, D.H., Foland, K.A., 1994. A short interval of Jurassic continental flood basalt volcanism in Antarctica as demonstrated by $^{40}\text{Ar}/^{39}\text{Ar}$ geochronology. *Earth Planet. Sci. Lett.* 121, 19–41.
- Helby, R., Morgan, R., Partridge, A.D., 1987. A palynological zonation of the Australian Mesozoic. In: Jell, P.A. (Ed.), *Studies in Australian Mesozoic Palynology*. Memoirs of the Association of Australasian Palaeontologists 4, 1–94.
- Hunter, M.A., Riley, T.R., Cantrill, D.J., Flowerdew, M.J., Millar, I.L., 2006. A new stratigraphy for the Latady Basin, Antarctic Peninsula: part 1, Ellsworth Land Volcanic Group. *Geol. Mag.* 143, 777–796.
- Jell, P.A. (Ed.), 2013. *Geology of Queensland*. Geological Survey of Queensland, Brisbane.
- Kerp, H., Bomfleur, B., 2011. Photography of plant fossils—new techniques, old tricks. *Rev. Palaeobot. Palynol.* 166, 117–151.
- Kyle, R.A., 1977. Palynostratigraphy of the Victoria Group of South Victoria Land, Antarctica. *N. Z. J. Geol. Geophys.* 20, 1081–1102.
- Kyle, R.A., Fasola, A., 1978. Triassic palynology of the Beardmore Glacier area of Antarctica. *Palinol. Número Extraordinario* 1, 313–319.

- Kyle, R.A., Schopf, J.M., 1982. Permian and Triassic palynostratigraphy of the Victoria Group, Transantarctic Mountains. In: Craddock, C. (Ed.), *Antarctic Geosciences*. The University of Wisconsin Press, Madison, pp. 649–659.
- McClintock, M., White, J.D.L., 2006. Large phreatomagmatic vent complex at Coombs Hills, Antarctica: wet, explosive initiation of flood basalt volcanism in the Ferrar–Karoo LIP. *Bull. Volcanol.* 68, 215–239.
- McKellar, J.L., 1978. Palynostratigraphy of samples from GSQ Eddystone 1. *Queensland Gov. Min. J.* 79, 424–434.
- McKellar, J.L., 1985. Biostratigraphy of spore-pollen floras from the Caloundra to Nambour area, Nambour Basin. *Queensland Gov. Min. J.* 86, 368–376.
- McKellar, J.L., in press. Late Early to Late Jurassic palynology, biostratigraphy and palaeogeography of the Roma Shelf area, northwestern Surat Basin, Queensland, Australia. *Memoirs of the Association of Australasian Palaeontologists*.
- Muirhead, J.D., Airoldi, G., Rowland, J.V., White, J.D.L., 2012. Interconnected sills and inclined sheet intrusions control shallow magma transport in the Ferrar large igneous province, Antarctica. *Geol. Soc. Am. Bull.* 124, 162–180.
- Musumeci, G., Pertusati, P.C., Ribecai, C., Meccheri, M., 2006. Early Jurassic fossiliferous black shales in the Exposure Hill Formation, Ferrar Group of northern Victoria Land, Antarctica. *Terra Antarctica Reports*, 12, pp. 91–98.
- Norris, G., 1965. Triassic and Jurassic miospores and acritarchs from the Beacon and Ferrar groups, Victoria Land, Antarctica. *N. Z. J. Geol. Geophys.* 8, 236–277.
- Pálffy, J., Smith, P.L., 2000. Synchrony between Early Jurassic extinction, oceanic anoxic events, and the Karoo–Ferrar flood basalt volcanism. *Geology* 28, 747–750.
- Pankhurst, R.J., Riley, T.R., Fanning, C.M., Kelley, S.P., 2000. Episodic silicic volcanism in Patagonia and the Antarctic Peninsula: chronology of magmatism associated with the break-up of Gondwana. *J. Petrol.* 41, 605–625.
- Pertusati, P.C., Ribecai, C., Carosi, R., Meccheri, M., 2006. Early Jurassic age for youngest Beacon Supergroup strata based on palynomorphs from Section Peak, northern Victoria Land, Antarctica. *Terra Antarctica Reports* 12, 99–104.
- Price, P.L., 1997. Permian to Jurassic palynostratigraphic nomenclature of the Bowen and Surat Basins. In: Green, P.M. (Ed.), *The Surat and Bowen Basins, South-east Queensland*. Queensland Minerals and Energy Review Series. Queensland Department of Mines and Energy, Brisbane, pp. 137–178.
- Price, P.L., Filatoff, J., Williams, A.J., Pickering, S.A., Wood, G.R., 1985. Late Palaeozoic and Mesozoic palynostratigraphical units. CSR Oil and Gas Division Palynology Facility Report 274/225. open file report CR14012. Department of Natural Resource and Mines.
- Raine, J.I., Beu, A.G., Boyes, A.F., Campbell, H.J., Cooper, R.A., Crampton, J.S., Crundwell, M.P., Hollis, C.J., Morgans, H.E.G., 2012. New Zealand Geological Timescale v. 2012/1. [An update of the NZ Geological Timescale (Cooper, 2004) incorporating revised ages from the 2012 International Geological Timescale (Gradstein et al., 2012) and recalibration of NZ stage boundaries: <http://www.gns.cri.nz/Home/Our-Science/Earth-Science/Fossils/Online-Resources/New-Zealand-s-Geological-Timescale>].
- Renne, P.R., Deino, A.L., Walter, R.C., Turrin, B.D., Swisher, C.C., Becker, T.A., Curtis, G.H., Sharp, W.D., Jaouin, A.-R., 1994. Intercalibration of astronomical and radioisotope time. *Geology* 22, 783–786.
- Reiser, R.F., Williams, A.J., 1969. Palynology of the Lower Jurassic sediments of the northern Surat Basin, Queensland. Geological Survey of Queensland Publication 339. *Palaeontological Paper*, 15 (24 pp.).
- Ribecai, C., 2007. Early Jurassic miospores from Ferrar Group of Carapace Nunatak, South Victoria Land, Antarctica. *Rev. Palaeobot. Palynol.* 144, 3–12.
- Riley, T.R., Knight, K.B., 2001. Age of pre-break-up Gondwana magmatism. *Antarct. Sci.* 13, 99–110.
- Riley, T.R., Leat, P.T., Pankhurst, R.J., Harris, C., 2001. Origins of large volume rhyolitic volcanism in the Antarctic Peninsula and Patagonia by crustal melting. *J. Petrol.* 42, 1043–1065.
- Schöner, R., Viereck-Goette, L., Schneider, J., Bomfleur, B., 2007. Triassic–Jurassic sediments and multiple volcanic events in North Victoria Land, Antarctica: a revised stratigraphic model. In: Cooper, A.K., Raymond, C.R., et al. (Eds.), *Antarctica: A Keystone in a Changing World* — Online Proceedings of the 10th ISAES. USGS Open-File Report 2007-1047, Short Research Paper, 102. <http://dx.doi.org/10.3133/of2007-1047.srp102> (5 pp.).
- Schöner, R., Bomfleur, B., Schneider, J., Viereck-Goette, L., 2011. A systematic description of the Triassic to Lower Jurassic Section Peak Formation in north Victoria Land (Antarctica). *Polarforschung* 80, 71–87.
- Shang, Y.-K., 1997. Middle Jurassic Palynology of Carapace Nunatak, Victoria Land, Antarctica. *Acta Palaeontol. Sin.* 36, 170–186.
- Stevens, J., 1981. Palynology of the Callide Basin, east-central Queensland. *University of Queensland Department of Geology Papers*, 9, pp. 1–35.
- Stevens, G.R., 2004. Hettangian–Sinemurian (Early Jurassic) ammonites of New Zealand. *N. Z. Geol. Surv. Paleontol. Bull.* 76, 107pp.
- Tasch, P., Lammons, J.M., 1978. Palynology of some lacustrine interbeds of the Antarctic Jurassic. *Palinol. Numero Extraordin.* 1, 455–460.
- Tessensohn, F., Mädlar, K., 1987. Triassic plant fossils from North Victoria Land, Antarctica. *Geol. Jahrb.* B66, 187–201.
- Tozer, E.T., 1988. Rhaetian: a substage, not a stage. *Albertiana* 7, 9–15.
- Viereck-Goette, L., Schöner, R., Bomfleur, B., Schneider, J., 2007. Multiple shallow level sill intrusions coupled with hydromagmatic explosive eruptions marked the initial phase of Ferrar Magmatism in northern Victoria Land, Antarctica. In: Cooper, A.K., Raymond, C.R., et al. (Eds.), *Antarctica: A Keystone in a Changing World* — Online Proceedings of the 10th ISAES. USGS Open-File Report 2007-1047, Short Research Paper, 104. <http://dx.doi.org/10.3133/of2007-1047.srp104> (5 pp.).
- White, J.D.L., McClintock, M.K., 2001. Immense vent complex marks flood-basalt eruption in a wet, failed rift: Coombs Hills, Antarctica. *Geology* 29, 935–938.
- Wörner, G., 1992. Kirkpatrick Lavas, Exposure Hill Formation and Ferrar Sills in the Prince Albert Mountains, Victoria Land, Antarctica. *Polarforschung* 60, 87–90.
- Zhang, W., Grant-Mackie, J.A., 2001. Late Triassic–Early Jurassic palynofloral assemblages from Murihiku strata of New Zealand, and comparisons with China. *J. R. Soc. N. Z.* 31, 575–683.